OXFORD

Mineral Compositions of Syn-collisional Granitoids and their Implications for the Formation of Juvenile Continental Crust and Adakitic Magmatism

Yuanyuan Xiao[1,2,]*, Shuo Chen[1,2,3], Yaoling Niu[2,4,5], Xiaohong Wang[1,2], Qiqi Xue[5], Guodong Wang[6], Yaijie Gao[1,2,3], Hongmei Gong[1,2], Juanjuan Kong[1,2,3], Fengli Shao[7], Pu Sun[1,2,3], Meng Duan[5], Di Hong[1,2,3] and Dong Wang[1,2,3]

[1]Key Laboratory of Marine Geology and Environment, Institute of Oceanology, Chinese Academy of Sciences, Qingdao 266071, China; [2]Laboratory for Marine Geology, Qingdao National Laboratory for Marine Science and Technology, Qingdao 266061, China; [3]University of Chinese Academy of Sciences, Beijing 100049, China; [4]Department of Earth Sciences, Durham University, Durham Dh1 3LE, UK; [5]School of Earth Science and Mineral Resources, China University of Geosciences, Beijing 100083, China; [6]Shandong Provincial Key Laboratory of Water and Soil Conservation and Environmental Protection, School of Resources and Environment, Linyi University, Linyi, 276000, China; [7]Institute of Geology and Paleontology, Linyi University, Linyi, 276000, China

*Corresponding author. Telephone: +86-0532-82898035. Fax: +86-0532-82898035.
E-mail: yuanyuan.xiao@qdio.ac.cn

ABSTRACT

Continentalcollision zones have been proposed as primary sites of net continental crustal growth. Therefore, studies on syn-collisional granitoids with mafic magmatic enclaves (MMEs) are essential for testing this hypothesis. The Baojishan (BJS) and Qumushan (QMS) syn-collisional plutons in the North Qilian Orogen (NQO) on the northern margin of the Tibetan Plateau have abundant MMEs in sharp contact with host granitoids, sharing similar constituent minerals but with higher modal abundances of mafic minerals in MMEs. The QMS host granitoids have high Sr/Y and La/Yb ratios, showing adakitic compositions, which are differentfrom the BJS granitoids. Based on bulk-rock compositions and zircon U-Pb age-dating, recent studies on these two plutons proposed that MMEs represent cumulates crystallized early from the same magmatic system as their host granitoids, and their parental melts are best understood as andesitic magmas produced by partial melting of the underthrusting upper ocean crust upon collision with some terrigenous sediments under amphibolite facies. Here, we focus on the trace-element geochemistry of the constituent mineral phases of both MMEs and their host granitoids of the QMS and BJS plutons. Weshow that different mineral phases preferentially host different trace elements; for example, most rare earth elements (REEs and Y) reside in titanite (only found in the QMS pluton), amphibole, apatite, epidote and zircon (mostly heavy-REEs); and high-field-strength elements (HFSEs) reside in biotite, titanite, amphibole and zircon. Based on the mineral chemical data, we show that for these two plutons, MMEs are of similar cumulate origin, crystallized from primitive andesitic melts in the early stage of granitoid magmatism. The primitive andesitic melts for these syn-collisional granitoids are most likely produced by the partial melting of the oceanic crust, supporting the hypothesis of continental crustal growth considering the syn-collisional granitoids represent juvenile continental crust. As evidenced by distinct mineral compositions, the two plutons have different parental magma compositions, for example higher TiO_2 content and higher Sr/Y and La/Yb ratios in the QMS parental magmas, a signature best understood as being inherited from the source. The higher TiO_2 content

of the parental magma for the QMS pluton leads to the common presence of titanite in the QMS pluton (absent in the BJS pluton), crystallization of which in turn controls the trace-element (REE, Y, Nb, Ta and others) systematics in the residual melts towards an adakitic signature. Therefore, parental magmas with high TiO_2 content and high Sr/Y and La/Yb ratios, as well as their further fractionation of titanite, are important factors in the development of adakitic compositions, as represented by the QMS host granitoids. This model offers a new perspective on the petrogenesis of adakitic rocks. The present study further demonstrates that, in general, mineral chemistry holds essential information for revealing the petrogenesis of granitoid rocks.

INTRODUCTION

The bulk continental crust is inferred to have been produced by the low-degree partial melting of the primitive mantle in the Earth's early history because of the compositional complementarity between incompatible element-enriched continental crust and incompatible element-depleted oceanic crust, the depletion of which is thought to be inherited from the upper mantle, depleted as the result of continental crust extraction (e.g., O'Nions *et al.*, 1979; Hofmann, 1988). However, how the continental crust with andesitic composition may have derived from mantle-derived basaltic magmas remains unclear. While it is widely accepted that island arcs are the main building blocks responsible for the growth of the continental crust (e.g., Taylor, 1967, 1977), considerable amounts of continental crustal materials have also been recognized to be lost during crustal destruction by subduction removal (e.g., Stein & Scholl, 2012). Meanwhile, the growth of the continental crust is episodic (e.g., Condie, 1998). Hence, the 'Island-arc' model (Taylor, 1967, 1977) may not be responsible for continental crustal growth. On the basis of studies of syn-collisional andesites and granitoids from southern Tibet (Niu *et al.*, 2007; Mo *et al.*, 2008), Niu *et al.* (2013) proposed that continental collision zones are primary sites for net continental crust growth. Importantly, Niu *et al.* (2013) demonstrated that syn-collisional andesites and granitoids show remarkable similarity to bulk continental crustal compositions in all the major and trace-element abundances and ratios, suggesting that syn-collisional granitoids represent juvenile continental crust resulting from the partial melting of the subducting/subducted upper oceanic crust with minor terrigenous sediments under amphibolite facies (Mo *et al.*, 2008; Niu & O'Hara, 2009; Niu *et al.*, 2013). Studies on the petrogenesis of syn-collisional granitoids are important for testing this hypothesis. Our studies on syn-collisional granitoids with mafic magmatic enclaves (MMEs) from orogens on the Tibetan Plateau and adjacent regions (e.g., Qinling, Kunlun and Qilian orogens) support this hypothesis in many respects, including significant mantle Nd-Hf isotopic contributions to the granitoids (Huang *et al.*, 2014, 2015, 2016, 2017; Chen *et al.*, 2015, 2016, 2018; Zhang *et al.*, 2016). Nevertheless, quantification is necessary in order to develop this testable hypothesis into a comprehensive theory. This requires refined experimental petrology on oceanic crust melting in the context of continental collision, and detailed major- and trace-element systematics in the constituent minerals of syn-collisional granitoids and the hosted MMEs.

As minerals are magmatic products, the mineralogy and mineral compositions hold the key to magmatic conditions and processes (e.g., Sha & Chappell, 1999; Belousova *et al.*, 2002a; Hoskin & Schaltegger, 2003; Piccoli *et al.*, 2011), such as oxygen fugacity (e.g., Belousova *et al.*, 2002b), magma mixing (McLeod *et al.*, 2011; Bruand *et al.*, 2014), fractional crystallization (Marks *et al.*, 2008) and subsequent metasomatism (e.g., Smith *et al.*, 2009). Comprehensive geochemical studies on both major and accessory minerals are thus necessary before the petrogenesis of igneous rocks can be genuinely understood (e.g., Bachmann *et al.*, 2005; Gao *et al.*, 2009). In this paper, we present mineral *in situ* trace-element data on two well-characterized syn-collisional granitoid plutons, namely the Baojishan (BJS) and Qumushan (QMS) plutons in the North Qilian Orogen (NQO) on the northern margin of the Tibetan Plateau (Chen *et al.*, 2015, 2016, 2018). Both QMS and BJS plutons have similarly abundant MMEs in sharp contact with host granitoids, but the QMS host granitoids show adakitic characteristics, which is different from the QMS MMEs and the BJS granitoids (Chen *et al.*, 2015, 2016). Although the adakitic QMS host granitoids have been interpreted as resulting from fractional crystallization of primitive andesitic magmas (Chen *et al.*, 2016), this model needs quantifying by considering detailed and specific controls of the various crystallized minerals in the granitoid systems. Our data provide further constraints on the petrogenesis of MMEs in the context of syn-collisional granitoid magmatism, and also help to explain why the QMS host granitoids have adakitic compositions while the BJS granitoids do not, offering new insights into the widely discussed and debated origin of adakite and adakitic rocks.

GEOLOGICAL BACKGROUND AND PETROLOGY

The NQO at the northern margin of the Tibetan Plateau is an early Palaeozoic suture zone formed through the subduction of the Qilian seafloor and subsequent collision between the Alashan Block and the Qilian-Qaidam Block (Fig. 1a,b; Song *et al.*, 2006, 2013, 2014a,b). It comprises the southern and northern ophiolite belts, separated by an island-arc igneous complex. The ophiolite in the southern belt is thought to represent the ocean crust formed at the ocean ridge, while the ophiolite in the northern belt is of a back-arc basin origin (Fig. 1a,b; Xia *et al.*, 2003, 2012; Xia & Song, 2010; Song *et al.*, 2013; Xiao *et al.*, 2013). The Qilian ocean basin is thought to have formed since *c.* 710 Ma, with a recorded seafloor subduction history between *c.* 520 and *c.* 440 Ma, just prior to continental collision (Song *et al.*, 2013). The BJS and QMS granitoid plutons are located in the northern ophiolite belt of the eastern NQO. Both BJS and QMS plutons show a zircon U-Pb crystallization age of *c.* 430 Ma (Chen *et al.*, 2015, 2016), which is consistent with the timing of continental collision (i.e., *c.* 440–420 Ma; Song *et al.*, 2009, 2013).

The BJS and QMS plutons contain abundant MMEs of varying shape and size (a few to tens of centimetres in diameter) in sharp contact with their host granitoids (Fig. 1c,d). The hosts of both plutons are granodioritic, mainly composed of plagioclase (*c.* 40–50 %) + quartz (*c.* 20–30 %) + biotite (*c.* 10–20 %) + amphibole (*c.* 5–10 %; Fig. 2). The MMEs are dioritic with the same mineralogy as their host, but have a finer grain size, greater modal amphibole, and less modal plagioclase and quartz, i.e., amphibole (*c.* 25–45 %) + biotite (*c.* 15–20 %) + plagioclase (*c.* 20–40 %) + quartz (*c.* 5–10 %; Fig. 2). Pyroxene is not found in the MMEs and their host granitoids in either pluton. Accessory minerals are mainly apatite, epidote, titanite, zircon, muscovite and K-feldspar, with varying modal abundances in both MMEs and their host plutons (Fig. 2). Among others, epidote is more common in the BJS pluton (especially in host granodiorites; e.g., Fig. 2a–c), while apatite is more common in the QMS pluton. Titanite (up to *c.* 500 μm in length) is only found in the QMS pluton (e.g., Fig. 2e–h). Apatite crystals are always euhedral. Epidote crystals are anhedral, and some of them occur as inclusions in amphibole. Titanite is anhedral and shows varying coloured patches.

ANALYTICAL METHODS

MMEs and their host granitoids of the QMS and BJS plutons were prepared as 60-μm-thick sections, and major and accessory minerals were analysed using laser-ablation inductively coupled plasma mass spectrometry (LA-ICP-MS) in the Laboratory of Ocean Lithosphere and Mantle Dynamics (LOLMD) at the Institute of Oceanology, Chinese Academy of Sciences. We used a 193-nm ultra-short pulse excimer laser ablation system (Analyte Excite produced by Photon-

machines Company) coupled with an Agilent 7900 ICP-MS instrument. Operation conditions of the LA-ICP-MS analysis are summarized in the Supplementary Data, Table DR2, which may be downloaded from http://www.petrology.oupjournals.org/ (see details in the caption of Fig. DR1). Considering the relatively homogeneous compositions of igneous minerals, a large spot size of 40 μm was used with a low energy density (4.72 J/cm^2) to ensure that fractionation with increasing ablation depths was minimized. During each run, 53 elements, including both major and trace elements, were analysed. Acquisition times for background (gas blank) and subsequent sampling were 25 and 50 s, respectively. The Agilent Chemstation was utilized for the acquisition of each individual analysis.

Off-line data reduction, including signal selection, drift correction and quantitative calibration, was done using ICPMSDataCal (Liu *et al.*, 2008; Lin *et al.*, 2016). For anhydrous minerals (feldspar, titanite and zircon), all the analysed elements in each run were normalized to 100% and calibrated using an ablation yield correction factor (AYCF; Liu *et al.*, 2008) based on analysis of multiple reference materials, i.e., NIST SRM 610, USGS BCR-2G, BIR-1G, BHVO-2G and a synthesized glass GSE-1G (Jochum *et al.*, 2005). For hydrous minerals (amphibole, biotite, epidote, apatite, muscovite and carbonate), we chose ^{42}Ca (for apatite and carbonate) and ^{28}Si (for silicate minerals) as the internal standards for data calibration, which were previously analysed using an electron probe micro-analyser (EPMA; Chen *et al.*, 2015, 2016). In some cases, we instead used mineral compositional data from the literature for rocks with similar composition and mineralogy to our rocks (Dahlquist, 2002; Tables DR3,4,6,7,9). Each batch of sample analysis started and ended with the analysis of the multiple reference materials (i.e., NIST SRM 610, USGS BCR-2G, BIR-1G, BHVO-2G and GSE-1G). Analysis of every five samples was bracketed with analysis of GSE-1G twice, with one analysis used for monitoring drift and applying drift correction (if any), and the other indicating the analytical precision and accuracy, i.e., within 5% and below 10% respectively for most analysed elements (Fig. DR1; recommended values are referred to GeoReM). During the analysis, we purposely chose spots of fresh areas and avoided other mineral inclusions to ensure representativeness of the analysed mineral compositions.

RESULTS

Mineral chemical data for both MMEs and their host granodiorites from both plutons are summarized in Tables DR3–9, and primitive mantle normalized trace-element data for these minerals are presented in Fig. 3b–h, with the primitive mantle normalized trace-element diagram for the average bulk rock compositions for comparison (Fig. 3a).
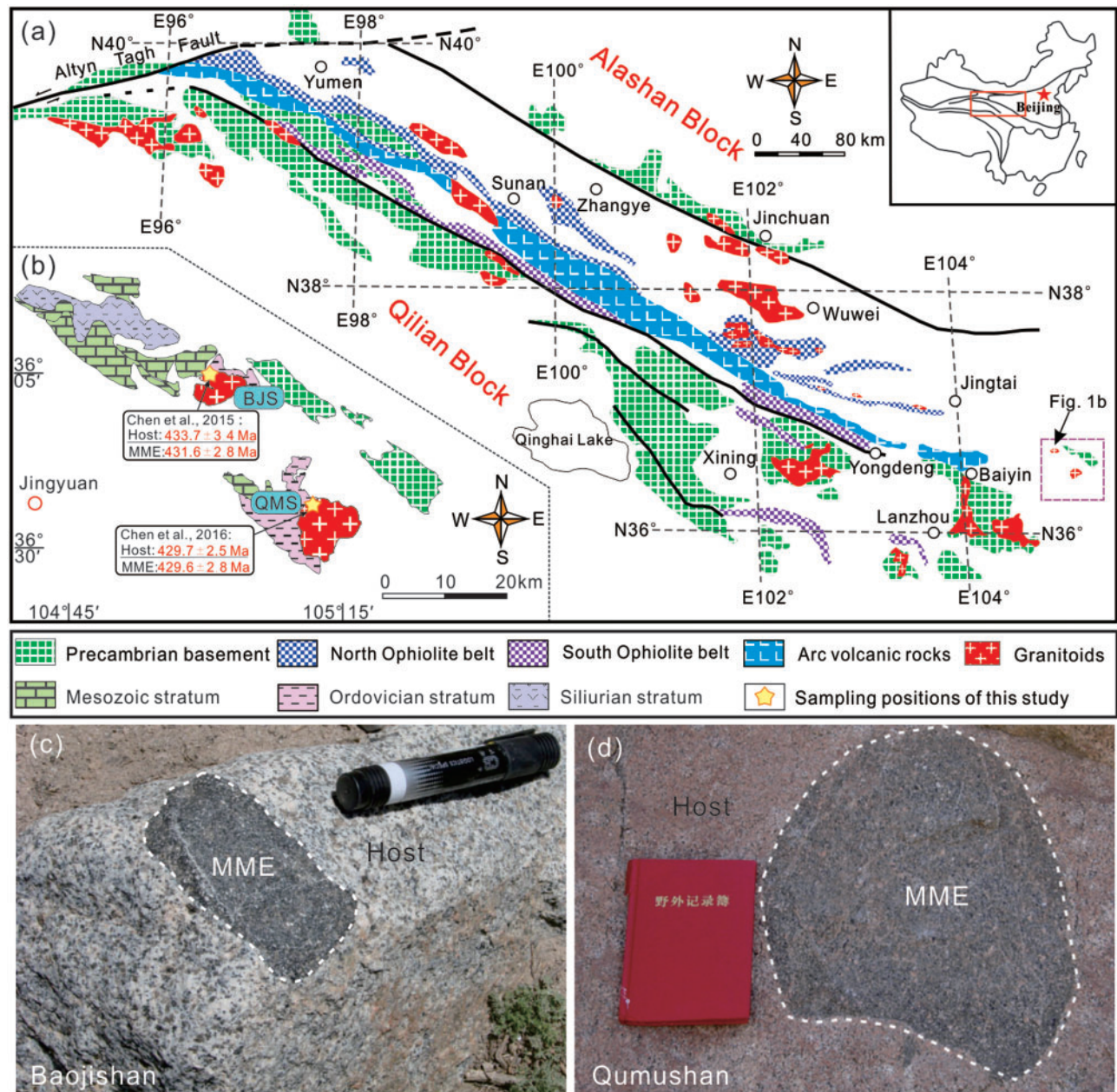
Fig. 1. (a-b) Geological map of NQO and sample locations for this study (after Chen *et al.*, 2015, 2016). (c-d) Field photos showing the sharp contact between host rocks and MMEs.

Amphibole

Amphibole from the QMS pluton has higher Mg# (63.2–70.4 vs 53.8–62.5) and lower Al_2O_3 (4.63–8.49 wt.% vs 7.33–10.56 wt.%) than that from the BJS pluton (Fig. 4; Table DR3). The QMS amphibole contains higher light rare earth elements (LREEs) and lower heavy rare earth elements (HREEs)-Y than the BJS amphibole (e.g., $[La/Yb]_N$ = 2.03–7.08 vs 0.19–1.81; Fig. 3b), consistent with greater LREE/HREE fractionation in the QMS bulk rocks (Fig. 3a and Table DR1). The QMS amphibole has higher Nb/Ta than the BJS amphibole (Figs. 3b, 4g and Table DR3). The QMS amphibole also has higher Ni and lower Sc contents than the BJS amphibole (Fig. 4h). Amphiboles in MMEs contain consistently higher Ni-Cr

and lower Sc than those of their host granitoids in both plutons (e.g., Fig. 4h) but share similar contents for most other analysed trace elements (Table DR3).

Biotite

Biotite from the QMS pluton shows higher Mg# (59.3–64.2 vs 52.6–58.6) and lower Al_2O_3 (13.45–15.22% vs 14.82–16.71%) than that of the BJS pluton (Fig. 5; Table DR4). Both QMS and BJS biotite contains high Ba-Rb-Cs-K, ~1000 times the primitive mantle values (Fig. 3c). The QMS biotite has somewhat higher LREEs-Sr contents and much lower Ta (Fig. 3c), with higher Nb/Ta ratios (Fig. 5a,b,d) than the BJS biotite (Table DR4). Furthermore, Nb/Ta ratios of biotite slightly decrease
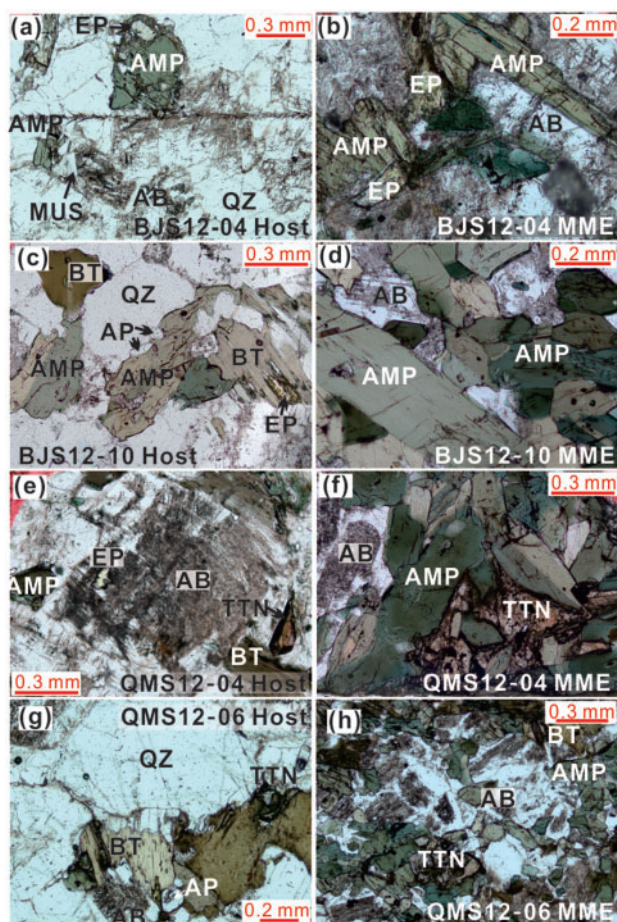
Fig. 2. (a-h) Photomicrographs for host granitoids (in the left column, i.e., a, c, e, g) and MMEs (in the right column, i.e., b, d, f, h) in pairs from the BJS and QMS plutons in the eastern NQO. (a-d) are for granitoids from the BJS pluton with more epidote; (e-h) are for granitoids from the QMS pluton with abundant titanite. Mineral abbreviations are: AB, albite; AMP, amphibole; AP, apatite; BT, biotite; EP, epidote; MUS, muscovite; QZ, quartz; TTN, titanite; ZRN, zircon. Primitive mantle values are from Sun & McDonough (1989).

rimwards (Fig. 5a,b). Some small muscovite crystals (Fig. 2a) were also analysed, and found to contain the highest Rb contents of all analysed minerals, up to 731 ppm (Table DR4). For both plutons, biotites from MMEs show a similar composition to those of their host granitoids (Table DR4).

Feldspar

Plagioclase An% (Ca/[Ca+Na+K]) values gently decrease towards crystal rims (Fig. 6a-d), and the QMS plagioclase has lower An values than that in the BJS pluton (Fig. 6e-h), 22% vs 39% on average (Table DR5). Plagioclase has high Pb, Sr, Ba, Cs and LREEs contents (Fig. 3c), which generally decrease with decreasing An (Fig. 6e–h), except for the gentle increase of Ba for the BJS plagioclase (Fig. 6f). Plagioclase in the QMS pluton shows obviously higher Ba-Cs-Sr and lower Y than that in the BJS pluton (e.g., Figs 3d, 6e–h), consistent with such differences in bulk rocks between the two plutons

(Fig. 3a; Table DR1). For both plutons, plagioclase from MMEs show similar compositions to those of their host granitoids (Fig. 3d; Table DR5).

Apatite

Apatite contains consistently high Th, U and REE contents, $\sim$1000 times the primitive mantle values (Fig. 3e). Apatite from the QMS pluton shows higher LREEs, lower HREEs and thus higher $[La/Yb]_N$ than that in the BJS pluton (Fig. 3e;Table DR6), which is consistent with what is observed in the bulk rocks (Fig. 3a; Table DR1).

Epidote

Epidote contains the highest Sr and Pb contents of all analysed minerals ($\sim$100 and $\sim$1000 times primitive mantle values, respectively; Fig. 3f). Because of small grain sizes, epidote in MMEs of the QMS pluton was not analysed. Epidote from the QMS host granitoids has higher Sr and LREEs and lower HREEs than that from the BJS pluton (Fig. 3f), consistent with the bulk-rock compositions (Fig. 3a).

Titanite

Titanite is only found in host and MMEs of the QMS pluton and has the highest Nb-Ta-Ti-Th-U-LREE contents of all minerals analysed, up to $\sim$10^4 times the primitive mantle values (Fig. 3g). Some titanite crystals show great variations in colour and composition, with firtree-like zoning or patches, and can be divided into two parts, namely more reddish parts and less reddish parts (Fig. 7). The more reddish parts show higher Nb-Ta-Zr-Hf-Th-U-Pb-REE-Y contents to variable extents (e.g., Figs 7, 8; Table DR8), but their LREE/HREE (e.g., La/Yb) and Th/U ratios generally overlap with those of the less reddish parts (Fig. 8d). No obvious titanite compositional differences exists between MMEs and their host rocks (Figs 3g, 8).

Others (zircon and carbonate)

Our in situ mineral analysis in thin sections (Table DR9) and previous analysis on zircon separates (Chen *et al.*, 2015, 2016; Table DR10) show that zircon has the highest Zr-Hf-HREE contents and the lowest $[LREE/HREE]_N$ among all the minerals analysed (Fig. 3h; Tables DR9, 10), e.g., $\sim$10^3 times the primitive mantle values for HREEs. Relative to the BJS zircon, the QMS zircon has generally higher Th-U-LREE contents, with relatively higher $[LREE/HREE]_N$ and Th/U ratios (0.7 vs 0.4 on average), and lower Eu/Eu* ($= Eu_N/[Sm_N \times Gd_N]^{1/2}$, 0.55 vs 0.61 on average) and Ce/Ce* values ($= Ce_N/[La_N \times Pr_N]^{1/2}$, 71 vs 125 on average; Fig. 3h; Tables DR9, 10). Some small carbonate crystals were analysed, showing high Sr (up to $\sim$400 ppm) and variably high LREEs and U (Table DR9).
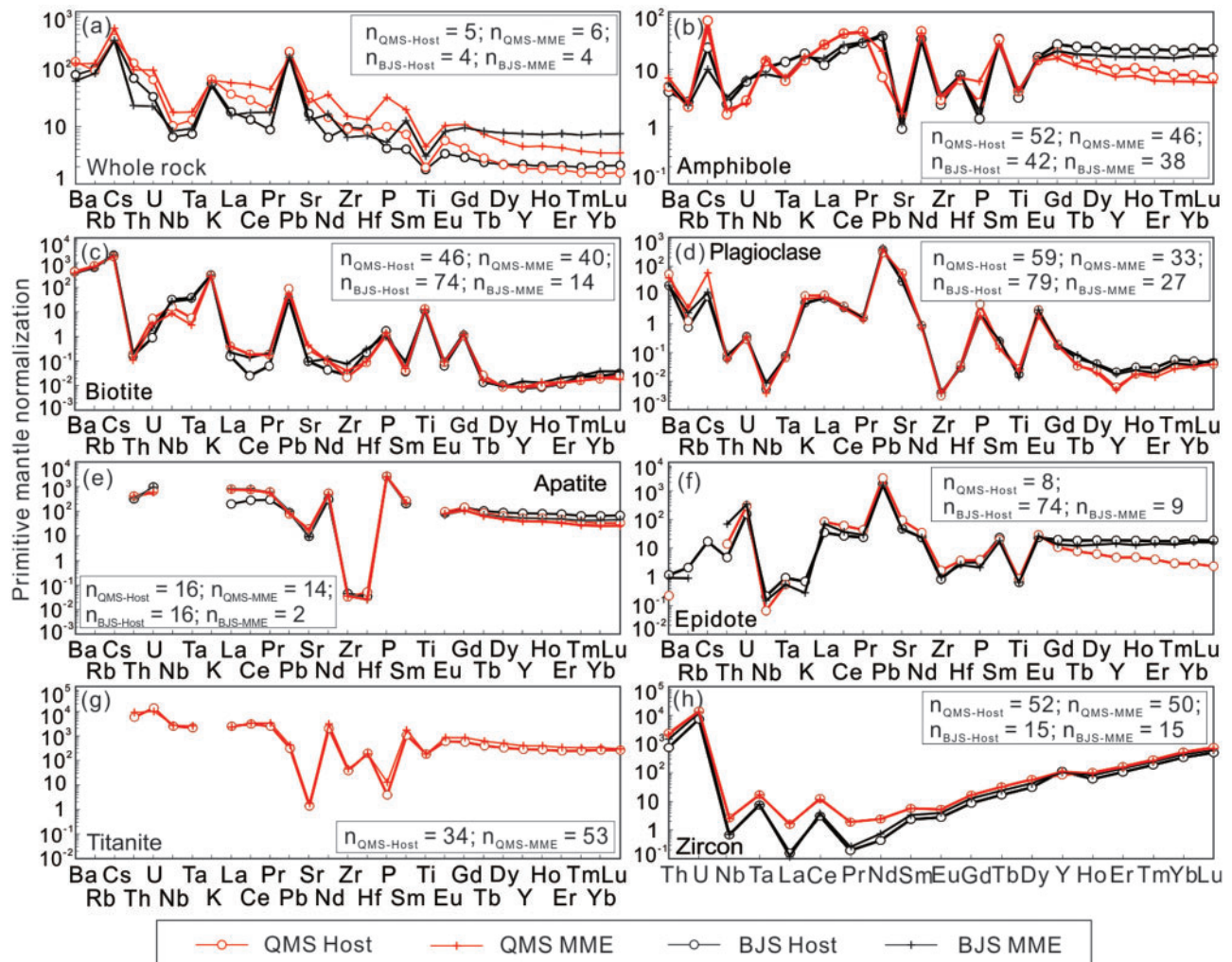
Fig. 3. (a) Primitive mantle (Sun & McDonough, 1989) normalized trace-element pattern for average bulk-rock compositions of MMEs and their host rocks from the BJS and QMS plutons (Chen *et al.*, 2015, 2016). (b-h) Primitive mantle (Sun & McDonough, 1989) normalized average mineral compositions of MMEs and their host granitoids from the QMS and BJS plutons, respectively.

DISCUSSION

Identifying trace-element budgets

Previous studies (mainly focused on titanite, apatite and zircon) have reported that accessory minerals can be significant trace-element hosts (especially for REEs and high-field-strength elements [HFSEs]; e.g., Sha & Chappell, 1999; Tiepolo *et al.*, 2002; Belousova *et al.*, 2002a,b; Hoskin and Schaltegger, 2003; Marks *et al.*, 2008; McLeod *et al.*, 2011; Piccoli *et al.*, 2011; Bruand *et al.*, 2014). To better understand how elements are controlled by different minerals, we reconstructed element budgets for average bulk-rock compositions of the MMEs and their host granitoids from the BJS and QMS plutons using average mineral compositions and modal mineralogy (Table DR11) normalized to averaged values of analysed element contents in bulk rocks (Fig. 9). Modal proportions for amphibole-plagioclase-biotite-epidote-apatite-titanite-carbonate-zircon were estimated using average bulk-rock major element contents through Cramer's rule (see details in Table DR11).

Considering that Si is the only major component for quartz, the proportion of quartz was simply calculated by using 1 minus the sum of other mineral proportions. The estimated mineral proportions are consistent with our petrologic observations, suggesting that both are reliable. Some large uncertainties for trace-element budgets are caused by uncertainties associated with modal estimation and mineral compositional variations at both crystal and bulk-rock scales. The compositional reconstruction in Fig. 9 is useful for understanding the trace-element distribution between phases (Table DR12) in the bulk-rock make-up, which is essential for correctly interpreting the petrogenesis.

Different trace elements have their phase preference. For example, elements K-Rb-Cs-Ba are dominantly hosted in biotite; Pb-Sr in feldspar and epidote; Th-U-REEs-Y mainly in amphibole, titanite (only found in the QMS pluton), apatite and epidote; Nb-Ta-Zr-Hf in titanite, zircon (also for some HREEs) and amphibole; and transition metals (e.g., Sc-V-Cr-Ni) mainly in amphibole
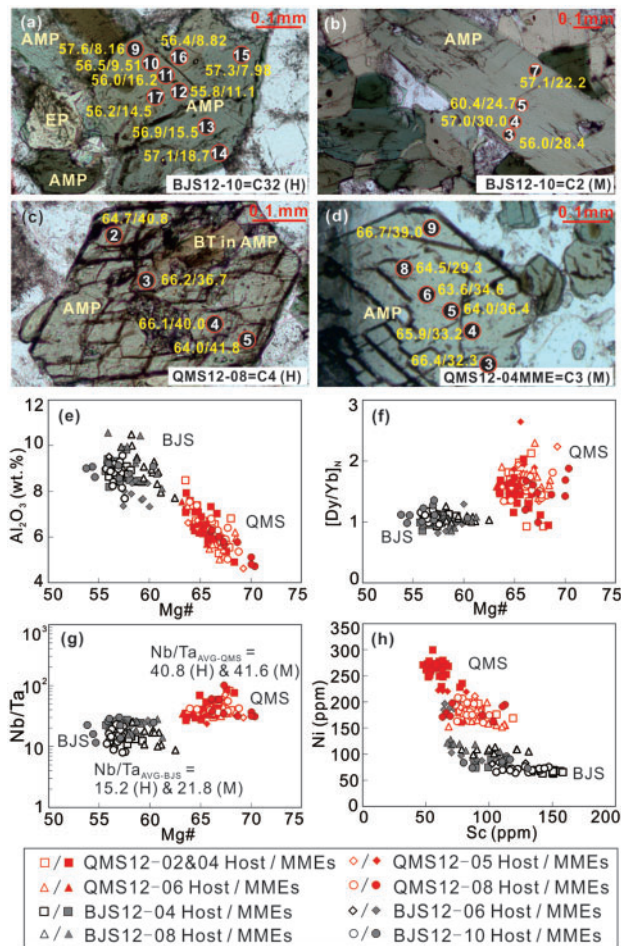
Fig. 4. (a-d) Mg# (= 100*Mg/[Mg+Fe^{2+}]) and Nb/Ta ratio profiles for amphibole in MMEs and their host granitoids from the BJS (a-b) and QMS (c-d) plutons. H, host; M, MME; AVG, average. Numbers are read as follows: for example, ⑧ 64.5/29.3 means that analytical spot 8 has Mg# = 64.5 and Nb/Ta = 29.3, given in Table DR3. (e-h) Elemental and ratio covariation diagrams for amphibole from the two plutons.

and biotite. Biotite is also an important host for Ti-Nb-Ta. All these findings indicate that accessory minerals, such as titanite, apatite, zircon and epidote, are as important as major minerals in hosting their preferred trace elements in bulk rocks. The understanding of trace element budgets forms the basis for understanding which mineral fractionation can control what geochemical variations during magma evolution. In the following, we use this knowledge to discuss the petrogenesis of MMEs and their host granitoids for the QMS and BJS plutons.

Genetic link between the QMS and BJS plutons and the formation of MMEs

Petrogenesis of MMEs and syn-collisional granitoids

Strictly speaking, granitoids, like other intrusive rocks, do not represent melts, but 'mechanical' mixtures of solidified 'interstitial' melts and crystalline phases (Niu, 2005). Hence, the bulk-rock composition of granitoids is
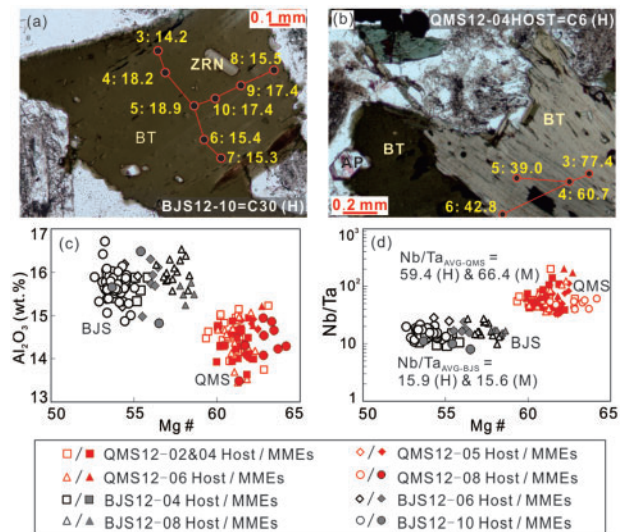

Fig. 5. (a-b) Nb/Ta ratio variation of biotite from the BJS and QMS plutons. Numbers are read as follows: for example, 8: 15.5 means that analytical spot 8 has Nb/Ta = 15.5, given in Table DR4. (c-d) Mg# variation diagrams for Al_2O_3 and Nb/Ta ratios of biotite from the two plutons.

largely determined by the type and mode of minerals present. It follows that mineral-mode controlled bulk-rock composition alone may not provide unique information on the parental magmas. Because minerals must be in equilibrium with the melt from which they crystallize, mineral compositions directly record the melt compositions. Therefore, both mineral chemistry and bulk-rock composition are required to constrain the petrogenesis of these granitoids and their MMEs, including the compositions of their parental magmas and magma sources, as well as the petrogenetic processes operating.

Both BJS and QMS syn-collisional granitoid plutons are situated in the eastern NQO (Fig. 1b). They were produced in the same tectonic setting through the same process and at the same time (the same zircon crystallization age of *c.* 430 Ma; Chen *et al.*, 2015, 2016). Specifically, the MMEs and host granitoids of both plutons have similar mineral assemblages, with more abundant mafic phases in MMEs than their host, and share similarly high contents of large-ion lithophile elements (LILEs) and low contents of HFSEs with relatively flat HREE patterns (Fig. 3a) and positive ε$_{Hf}$ (t) values (Chen *et al.*, 2015, 2016). Based on these geochemical features, Chen *et al.* (2015, 2016) concluded that primitive magmas parental to both plutons resulted from the partial melting of the underthrusting upper oceanic crust upon collision, with minor terrigenous sediment contributions under amphibolite facies (Niu *et al.*, 2013; Fig. 10).

Regarding the formation of MMEs, various models have been proposed in the literature. The MMEs are thought to represent mantle-derived basaltic magmas mixing with granitic magmas (e.g., Vernon, 1984; Chen *et al.*, 2009; McLeod *et al.*, 2011; Bruand
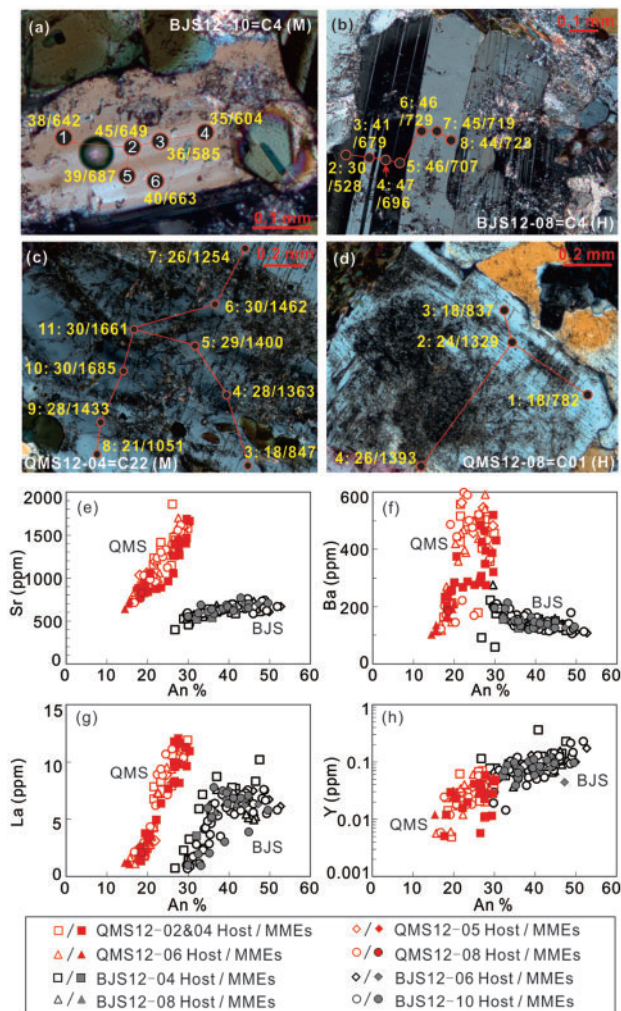
Fig. 6. (a–d) Anorthite and Sr content variation for plagioclase in MMEs and their host granitoids from the BJS (a–b) and QMS (c–d) plutons. Numbers are read as follows: for example, ⑧ or 8: 44/723 means that analytical spot 8 has An = 44 and Ba = 723 ppm, given in Table DR5. (e-h) An-variation diagrams for Sr, Ba, La and Y of plagioclase from the two plutons.

et al., 2014), refractory restite after granitic magma extraction (e.g., Chappell and White, 1991), or early crystallized mafic cumulate fragments dispersed in the cogenetic granitic magmas (e.g., Dahlquist, 2002; Niu *et al.,* 2013). Specifically, for the BJS and QMS plutons, the compositional similarity of minerals from MMEs and their host granitoids shown in this study (Figs 3–8) indicates that both the MMEs and their host granitoids share common parental magmas, with their mineral compositions strongly dependent on parental magma compositions. The generally overlapping mineral compositions are inconsistent with MMEs being of restite origin or external origin. Furthermore, the relatively uniform compositions for all the analysed individual mineral crystals (i.e., rather weak core-to-rim variations without complex zoning; Figs 4–7) indicate the absence of disequilibrium, arguing against a magma-mixing origin of the MMEs (Browne *et al.,* 2006; Chen *et al.,* 2009; Bruand *et al.,* 2014; McLeod *et al.,* 2011). Hence, our new mineral data

support the idea that MMEs and respective host granitoids share the same parental magmas. This is consistent with the results of previous studies (Chen *et al.,* 2015, 2016) on bulk-rock geochemistry (e.g., uniform Sr-Nd-Hf isotopic composition) and the same zircon U-Pb age of MMEs and host granitoids for these two plutons.

Our studied MMEs show a finer grain size than their host granitoids, which is in fact consistent with an earlier cumulate origin of the same magmatic systems if we consider the process of magma emplacement, 'magma chamber' development and evolution (Fig. 10). When the primitive magmas intrude into the 'cold' crust to develop a magma chamber, rapid cooling can significantly enhance crystal nucleation and result in the crystallization of fine-grained cumulates dominated by mafic minerals near the walls and base of the magma chamber. These fine-grained cumulates are later dispersed as MMEs in the slowly cooling magma bodies that solidified as the coarse-grained granitoid host. Hence, fine-grained MMEs of cumulate origin can be present in the host granitoid through this process.

Despite the similarities in bulk-rock incompatible element patterns (Fig. 3a) and mineral compositions (Figs 3–8) between MMEs and host granitoids as a result of their having the same parental magma, MMEs also show some compositional differences from their host granitoids in the BJS and QMS plutons, for example significantly higher middle (M)-HREE contents (Fig. 3a) and Sc-V-Cr-Ni (Table DR1). These differences are in fact controlled by their high modal amphibole content, as these elements are less incompatible in amphibole (e.g., Bottazzi *et al.,* 1999; Tang *et al.,* 2017; Zhang *et al.,* 2019), which is consistent with amphibole being the primary host mineral for M-HREEs in our modelling results (Table DR11; Fig. 9), and our petrologic observations (Fig. 2). The slight differences of LREEs between MMEs and host granitoids from the QMS (Fig. 3a) are caused by titanite, which is present only in the QMS. Hence, bulk-rock REE variations between MMEs and their host granitoids for both the QMS and BJS plutons are controlled by different modal abundances of amphibole (and also titanite for the QMS pluton), i.e., higher modes of amphibole and titanite for higher contents of REEs in the MMEs. Similarly, the bulk-rock variations of Sc-V-Cr-Ni between MMEs and their host granitoids for the two plutons (Table DR1) result from the varying modal abundances of amphibole and biotite, which are the most important minerals for hosting these elements (Fig. 9). All of these chemical characteristics are consistent with the much stronger fractionation of these minerals (e.g., amphibole, biotite) at earlier stages of magma evolution, in support of MMEs representing the early cumulate formed from the same magmatic system, followed by the formation of their host granitoids.

Implications for continental crustal growth
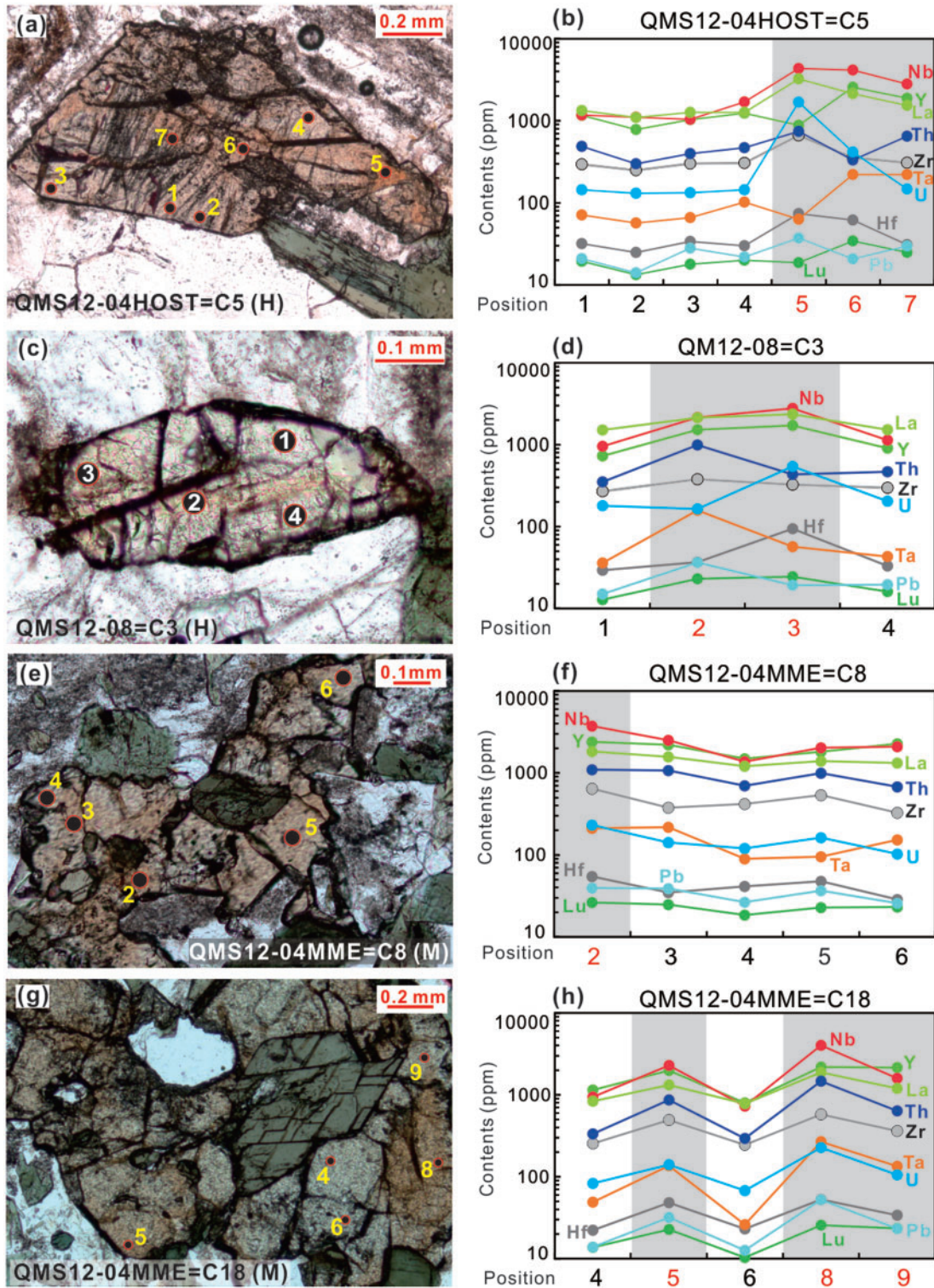Experimental studies have shown that Fe/Mg ratios of amphibole positively correlate with that of their

Fig. 7. Titanite compositional variation for the BJS and QMS plutons. Analytical spot numbers in both the left and right panels are as given in Table DR8. The position numbers highlighted in red in the right panels represent those analysed points with more reddish colour, the element contents of which plot in grey areas, as indicated in the right panels. This shows that the more reddish parts tend to have higher Nb-Ta-Zr-Hf-Th-U-Pb-La (LREE)-Lu (HREE).

equilibrium andesitic melt, and that the amphibole Mg# ($100 \times$ molar [Mg/(Mg+Fe)]) systematically decreases with decreasing temperature during magma fractionation for both low- and high-pressure conditions

(Alonso-Perez *et al.*, 2009). Thus, the amphibole Mg# can be used to evaluate the Mg# and degree of fractionation of the equilibrium melt, which reflects whether amphibole formed from primary basaltic melts or
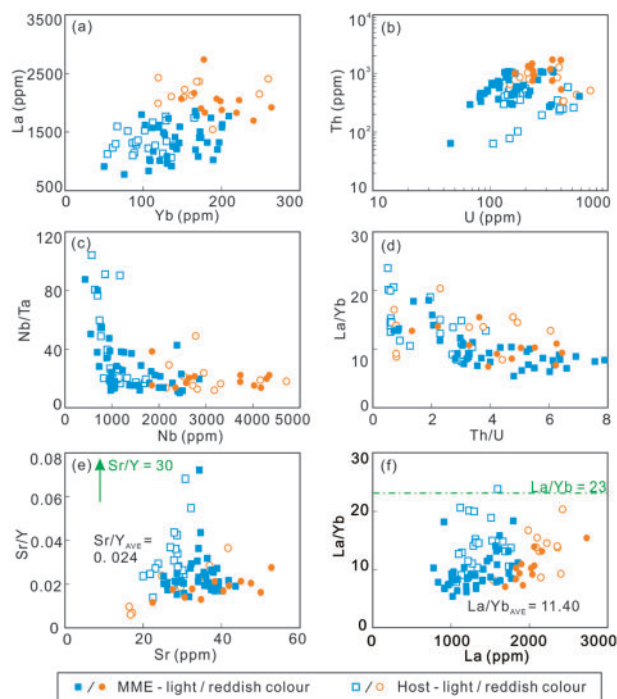
Fig. 8. Elemental and ratio covariation diagrams for titanite from the QMS pluton. In (e-f), the modelled bulk parental magma composition using the average composition of amphibole in MMEs of the QMS pluton (Sr/Y = 30, La/Yb = 23) is also plotted, for comparison. The extremely low Sr/Y and La/Yb ratios of titanite relative to those of the bulk parental magma indicate that the fractionation of titanite can effectively increase these ratios in the residual melts.

andesitic melts (Carmichael, 2002; Hidalgo & Rooney, 2010; Rooney *et al.*, 2011; Tiepolo *et al.*, 2012; Ribeiro *et al.*, 2016).

The overlapping Mg# values of our analysed amphibole from MMEs and host granitoids also indicate the same parental magma for MMEs and host granitoids in each pluton (Fig. 4). These analysed Mg# values (i.e., 63–70 for the QMS amphibole and 54–63 for the BJS amphibole) overlap with those of the liquidus amphiboles in experiments on andesitic melts (< 65; Alonso-Perez *et al.*, 2009; Prouteau and Scaillet, 2013), indicating that the MMEs and host granitoids of the two plutons are derived from andesitic melts. Although andesitic melts can also result from the evolution of basaltic melts, the observed mineral assemblage of amphibole and feldspar without pyroxene, together with the positive ε_{Hf} (t) values (mantle signature) of these rocks (Chen *et al.*, 2015, 2016) and recent modelling for the fractionation effects of NQO syn-collisional granitoids (Chen *et al.*, 2018) suggest that parental magmas for syn-collisional granitoids from these two plutons are most likely primitive andesitic melts. Importantly, the volume of andesitic melts as the result of basaltic magma evolution is minor, and the fractionation of basaltic magmas cannot produce volumetrically significant (of the order of $\sim 10^5$–10^6 km^3) syn-collisional granitoids along each and every orogenic

belt we studied, nor globally (Niu, 2005; Niu *et al.*, 2013). Hence, our new data on mineral compositions further support that these syn-collisional granitoids result from primitive andesitic magmas produced by partial melting of the underthrusting oceanic crust in response to continental collision (Fig. 10), which can contribute to the net continental crust growth if these syn-collisional granitoids are preserved in continental collision zones (Mo *et al.*, 2008; Niu & O'Hara, 2009; Niu *et al.*, 2013; Chen *et al.*, 2015, 2016, 2018).

Geochemical differences between the QMS and BJS plutons and the adakitic characteristics of the QMS host granitoids

Compositionally distinct parental magmas for the two plutons

Although the QMS and BJS plutons share a common tectonic setting in space and time as discussed above, bulk-rock compositions of the QMS granitoids and MMEs are clearly different from those of the respective BJS granitoids and MMEs; for example, the QMS granitoids and MMEs have higher Mg#, TiO$_2$, REEs, and HFSEs with higher LREE/HREE ratios and lower CaO (Fig. 3a and Table DR1; Chen *et al.*, 2015, 2016). The same mineral phases in the two plutons also show systematic differences accordingly (Figs 4–6, 11). Amphibole and biotite in the QMS pluton have higher Mg# (Figs 4–5), while feldspar exhibits lower An % (Fig. 6). The REE-hosting minerals (i.e., amphibole, apatite, epidote and zircon) in the QMS pluton show generally higher LREE/HREE ratios than those in the BJS pluton (Figs 3, 11). Biotite and amphibole, which are important hosts for Nb and Ta, in the QMS plutons have similar Nb contents but variably lower Ta contents than those in the BJS pluton (Tables DR3, DR4), resulting in characteristically higher Nb/Ta ratios of these two minerals from the QMS pluton (Figs 3b,c, 4g, 5d). Hence, the bulk-rock chemical differences between MMEs and host granitoids are controlled by varied modal mineralogy as a consequence of magma evolution (e.g., more amphibole crystallized in MMEs responsible for higher REE contents of MMEs), while it is the mineral compositional differences between QMS and BJS plutons that determine the bulk-rock compositional differences between the two plutons. Because mineral compositions record the compositions of melts in equilibrium with the minerals, these systematic mineral compositional differences (e.g., Figs 3–8) indicate that the two plutons evolved from compositionally different parental magmas.

Because amphibole as the liquidus phase has a 'similar' chemistry to andesitic magmas, it can be used to constrain the parental melt compositions (Hidalgo *et al.*, 2007; Tiepolo *et al.*, 2012; Chambefort *et al.*, 2013; Ribeiro *et al.*, 2016; Tang *et al.*, 2017). Considering the effect of melt compositions, we used partition coefficients between amphibole and basaltic-andesitic melts (data sourced from https://earthref.org/GERM/ and Hidalgo *et al.*, 2007; Table DR13) to calculate trace-element compositions of the melt in equilibrium with the amphibole. The calculated compositions of melt in equilibrium with
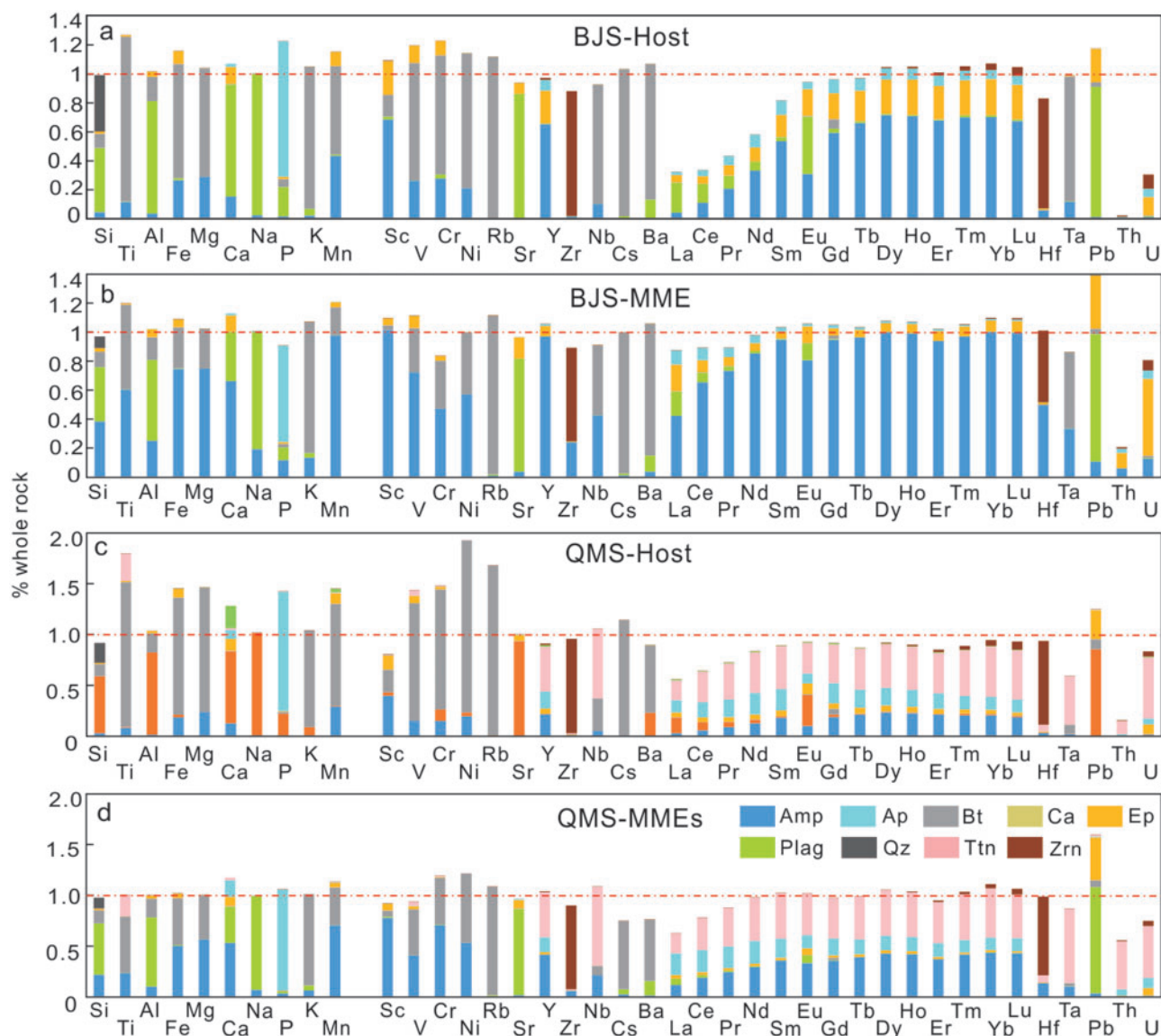
Fig. 9. Reconstructed elemental budgets in bulk-rock MMEs and their host rocks from the BJS and QMS plutons, normalized against their average bulk-rock compositions (Table DR1). '% whole rock' = 100% * $\sum_{i=1, j=1}^{i=m, j=n} X_i Y_j / Z_j$, where *i* refers to different mineral phases, *j* refers to different chemical elements, *X* refers to modelled mineral modal proportions (Table DR11), *Y* refers to the average content of chemical element *j* in analysed mineral *i* (Tables DR3-9), and *Z* refers to the average content of chemical element *j* in analysed bulk-rock samples (Table DR1), as indicated by the red dot-dashed lines in each panel. Bars with different colours represent different mineral hosts.

the QMS amphibole show greater REE fractionation (e.g., give the range of $[La/Yb]_N > 7.58–26.4$ vs 0.72–6.75 for the BJS equilibrium melt) and higher Sr/Y ratios than those for the BJS pluton (Figs 12, 13). Therefore, this further demonstrates that the andesitic magmas parental to the two plutons are distinctly different, reflecting compositional differences of their magma source.

The adakitic characteristics of the QMS host granitoid

'Adakite' is defined by its distinctive geochemical signatures, i.e., high SiO_2 ($\geq$ 56 wt %), Al_2O_3 ($\geq$ 15 wt %), Sr (> 400 ppm), Sr/Y (> 40) and La/Yb ratios (> 20), low Y (<18 ppm) and HREEs (Yb < 1.9 ppm), and was originally thought to be produced by the melting of young (no older than 25 Ma) and warm subducting oceanic crust under eclogite or garnet amphibolite facies conditions (Defant & Drummond, 1990). However, recent studies have found that adakitic rocks can be produced in different tectonic settings through different geological processes, for example the mixing of basaltic and felsic magmas (Chen *et al.*, 2013; Streck *et al.*, 2007), melting of mafic lower crust (Gao *et al.*, 2004; Chung *et al.*, 2003), and fractional crystallization of parental basaltic magmas (e.g., Castillo *et al.*, 1999, 2012; Wang *et al.*, 2005, 2007; Macpherson *et al.*, 2006; Rodríguez *et al.*, 2007; Ribeiro *et al.*, 2016).
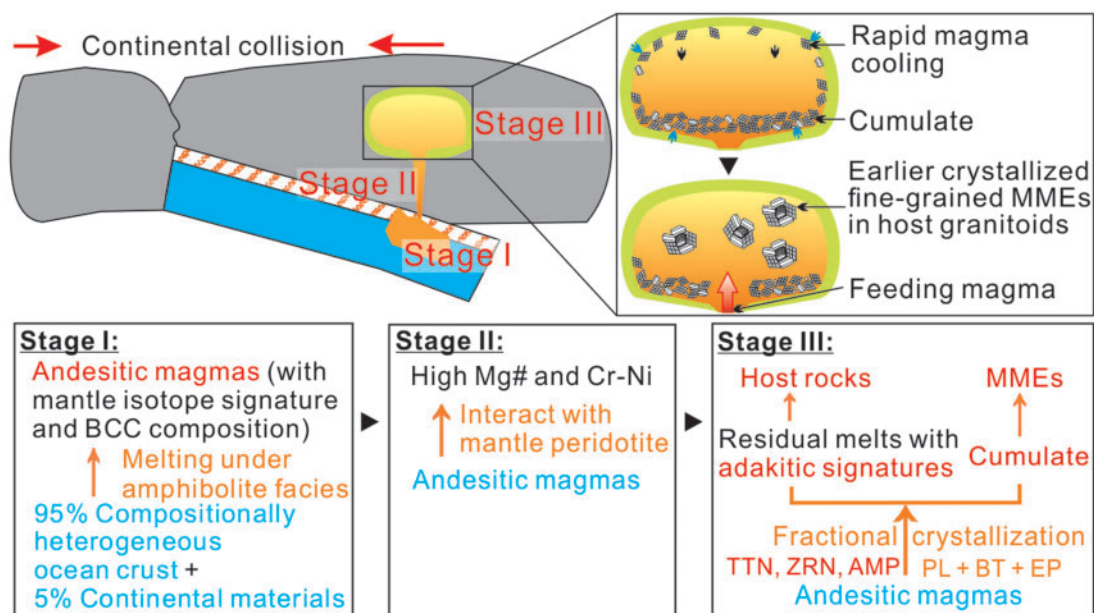
Fig. 10. Cartoon illustrating the petrogenesis of MMEs and host rocks. The development of MMEs in the context of the syn-collisional granitoid magma generation and evolution can be generalized in three stages (Niu *et al.*, 2013; Chen *et al.*, 2015, 2016, 2018): Stage I – compositionally heterogeneous ocean crust plus some terrigenous sediments melt to produce andesitic magmas during the continental collision under amphibolite facies conditions; Stage II – such magmas interact with mantle peridotite during ascent; Stage III – the andesitic magmas intrude into the 'cold' crust to develop a magma chamber, with the rapid cooling resulting in the crystallization of fine-grained cumulate dominated by mafic minerals near the walls and base of the magma chamber, to be later dispersed as MMEs in the slowly cooling magma bodies that solidified as the granitoid host. Among other minerals, the fractionation of titanite, zircon and amphibole will lead to a significant increase in Sr/Y and La/Yb ratios as observed in host rocks, which may lead to the formation of adakitic signatures as displayed by the QMS host rocks. BCC, bulk continent crust.

The QMS host granitoids show adakitic characteristics, i.e., high Sr/Y and La/Yb ratios (89 and 33 on average, respectively; Fig. 13 and Table DR1), which is different from the QMS MMEs and the BJS granitoids. In this study, we discuss detailed and specific controls of all the crystallized minerals such as amphibole, plagioclase, biotite, apatite, zircon, titanite, epidote in the granitoid systems, as illustrated in Fig. 13. The bulk-rock MMEs and host granitoids of the QMS pluton consistently show higher Sr/Y and La/Yb ratios than those of the BJS pluton (Fig. 13; Chen *et al.*, 2015, 2016), which is also true for their constituent minerals (e.g., amphibole, biotite, plagioclase and apatite; Figs 11, 13d, Tables DR3–9). In Fig. 13, the high Sr/Y and La/Yb ratios of the calculated melts in equilibrium with the MME amphiboles for the QMS pluton resemble adakitic compositions, while those for the BJS pluton do not, reflecting that the parental magma of the QMS pluton had high Sr/Y and La/Yb ratios. Thus, the systematic differences of Sr/Y and La/Yb ratios in both bulk-rock and mineral compositions between the two plutons (Figs 11–13) must have been inherited from their different parental magmas. All these observations demonstrate explicitly that the compositions of parental magmas exert a primary control on whether they have the potential to evolve to adakitic compositions.

Despite the relatively higher Sr/Y and La/Yb ratios of the parental magma for the QMS pluton, it is the host granitoid, not the MMEs, of the QMS pluton that clearly shows adakitic characteristics (Fig. 13a,b; Table DR1). The Sr/Y and La/Yb ratios of MMEs are lower than their parental magmas (Fig. 13a,b). This is consistent with the understanding that the MMEs do not represent melt compositions but are of cumulate origin. This, in turn, indicates that primitive andesitic melts parental to the QMS granitoid with high La/Yb and Sr/Y can further evolve into adakitic melts through fractional crystallization of the MME mineral assemblage. This MME fractionation that leads to adakitic melts is modelled in Fig. 13. For this, we (1) assume that the parental andesitic melts are in equilibrium with the MME amphibole of the QMS pluton, (2) apply Rayleigh fractional crystallization, and (3) use the modelled mineral modal abundances in the QMS MMEs (Table DR11) to approximate the co-precipitating phase assemblage of 25% amphibole + 45% plagioclase + 20% biotite + 1.7% apatite + 0.5% titanite + 2.4% epidote + 0.03% zircon, which is generally consistent with the petrographic observation (Fig. 2). Note that the bulk-rock compositions of the MMEs and samples of their host granitoid plot in complement with respect to the model parental melt, which is best illustrated in Fig. 13a.

Modelling shows that about 20% fractionation of the melts can produce the high Sr/Y and La/Yb ratios observed in the QMS host rocks (Fig. 13). Considering the mineral fractionation model in Fig. 13a, 0.1–0.2 % titanite fractionation is enough to increase Sr/Y ratios in the melts to be as high as in the QMS host rocks, which
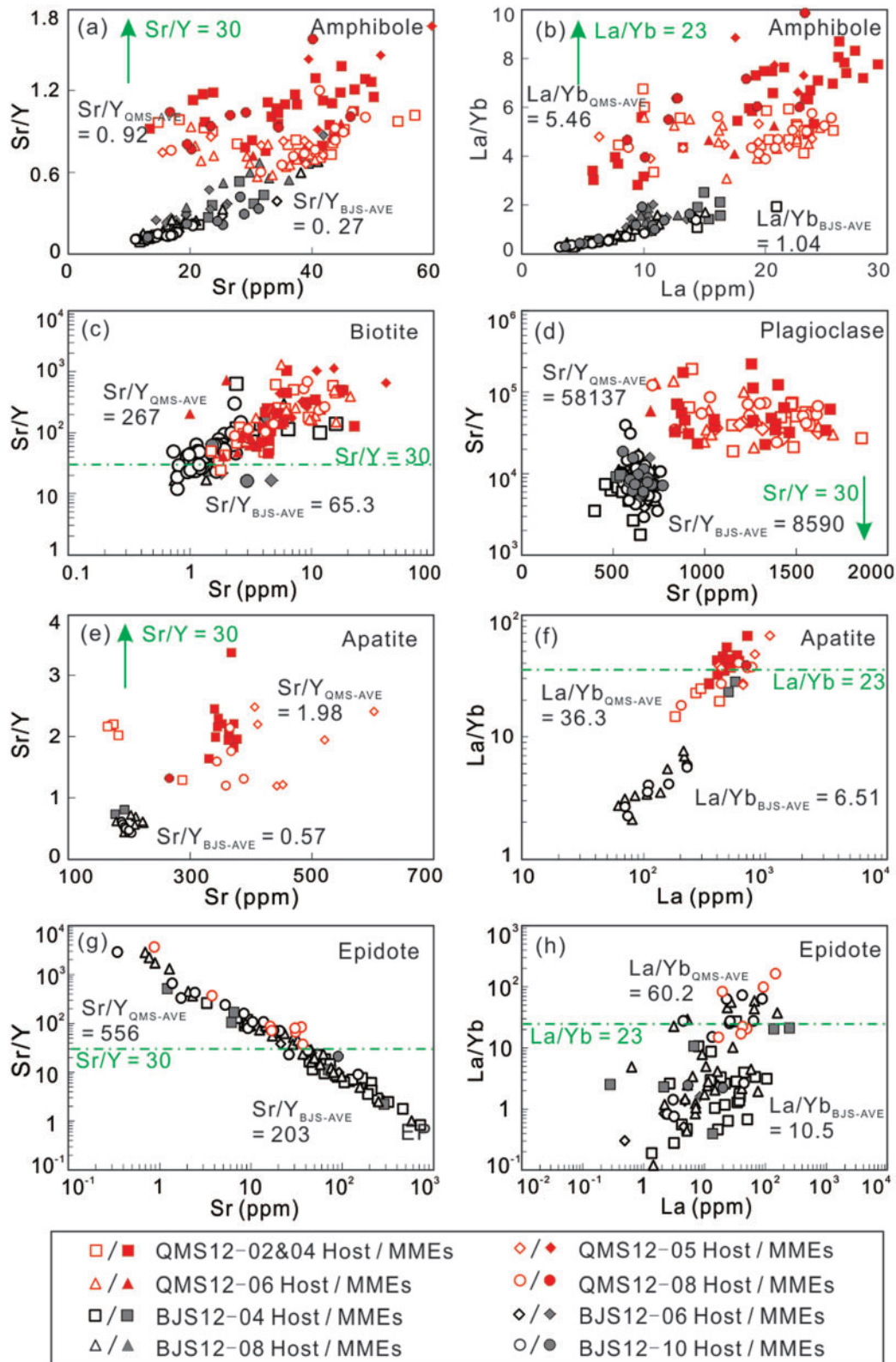
Fig. 11. Covariation diagrams for Sr/Y vs Sr, and La/Yb vs La for various minerals in the BJS and QMS plutons. The parental magma composition calculated using the average composition of amphibole in the QMS MMEs (Sr/Y = 30, La/Yb = 23) is also indicated for comparison. Notably, fractionation of those minerals with lower Sr/Y and La/Yb ratios than the bulk parental magma will increase these two ratios in the residual melts.
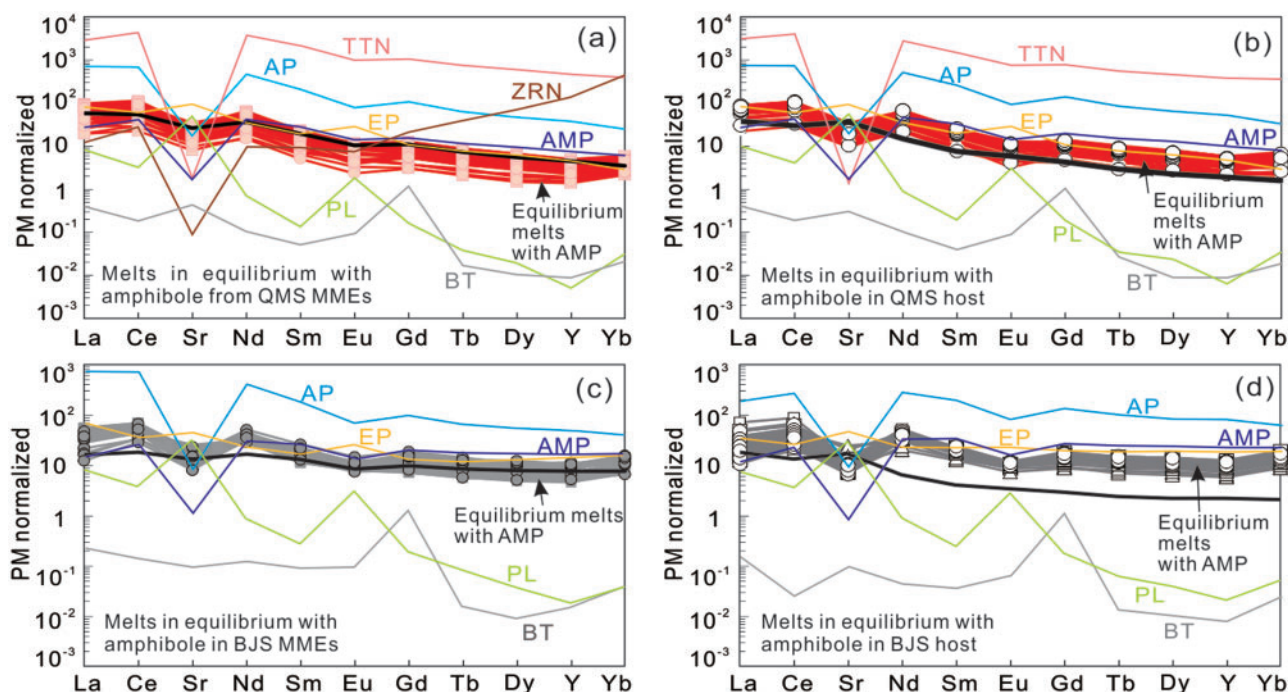
Fig. 12. Primitive mantle (PM; Sun & McDonough, 1989) normalized trace-element abundances for calculated compositions of melt in equilibrium with amphibole from MMEs and their host rocks of the BJS and QMS plutons, respectively. The thick black lines are the average bulk-rock compositions of MMEs and their host granitoids from the two plutons, respectively. Average mineral compositions in Tables DR3–9 are also plotted to indicate the contribution of various minerals.

is consistent with the very low Sr/Y ratios of titanite (~0.02; Fig. 13d and Table DR8) and its relatively common presence in the QMS pluton (Fig. 2e–h). Amphibole (< 40%) and zircon (< 1%) fractionation can also lead to the increase of Sr/Y ratios in the melts to as high as the values of the QMS host rocks (Fig. 13a). The effect of apatite fractionation is insignificant; that is, ~5–7% apatite is required to increase Sr/Y ratios in the melts to be similar to the values of the QMS host rocks (Fig. 13a), which is not supported by apatite modal abundances (no more than 2% based on the analysed P_2O_5 contents of bulk rocks, Table DR11). In addition, considering that zircon (with $[La/Yb]_N \ll 1.0$) and titanite have the highest Yb contents (up to hundreds of ppm) among all the minerals analysed (Fig. 3 and Tables DR8,9), 0.2% titanite or zircon can lead to the increase of La/Yb ratios to be as high as in the QMS host rocks (Fig. 13b). No more than 40% amphibole fractionation will result in the observed increase of La/Yb ratios in the melts. All of these are consistent with our modelled mineral modal abundances of the QMS MMEs (Table DR11) and much lower Sr/Y and La/Yb ratios of these minerals than in primitive melts parental to the QMS pluton (Figs 8e,f, 11, 13d). Furthermore, Eu/Eu* values of the melts can also increase correspondingly with the fractionation of titanite (0.2 %), according to the Eu/Eu* difference we observed between MMEs and their host granitoids of the QMS pluton (Fig. 13c).

Considering the distinction of mineral assemblages between the two plutons, namely the common presence of titanite in the QMS pluton and the absence of

titanite in the BJS pluton (Table DR11), our data indicate that the fractionation of titanite is the most important mineral to effectively increase both Sr/Y and La/Yb ratios in the residual melts and is most likely required for the formation of the adakitic characteristics of the QMS host rocks (Figs 10, 13). Although amphibole fractionation can also result in the increase of Sr/Y and La/Yb ratios in the residual melts, the higher degree of amphibole fractionation in the BJS pluton than in the QMS pluton (e.g., 44% vs 25% in MMEs in the modelling, Table DR11) is expected to result in even greater increases of Sr/Y and La/Yb ratios, which are inconsistent with the observed lower Sr/Y and La/Yb ratios in the BJS host granitoids (Fig. 13a,b). Thus, the effect of the amphibole fractionation in causing the adakitic signatures is not as important as that of the titanite fractionation. Although plagioclase crystallization will tend to decrease La/Yb and especially Sr/Y ratios in the residual melts, its effect on these ratios may have been suppressed by the fractionation of other minerals such as titanite and amphibole (Fig. 13).

Titanite crystallization may be controlled by magmatic conditions. However, because both BJS and QMS granitoids were produced by partial melting of the underthrusting oceanic crust in response to continental collision under the amphibolite facies at the same time, it is more likely that the QMS and BJS pluton share similar magmatic conditions. Using Al^T (i.e., Al content on tetrahedral site, which is sensitive to pressure) and Na + K (a temperature-sensitive indicator) of amphibole, Chen *et al.* (2018) have shown that most
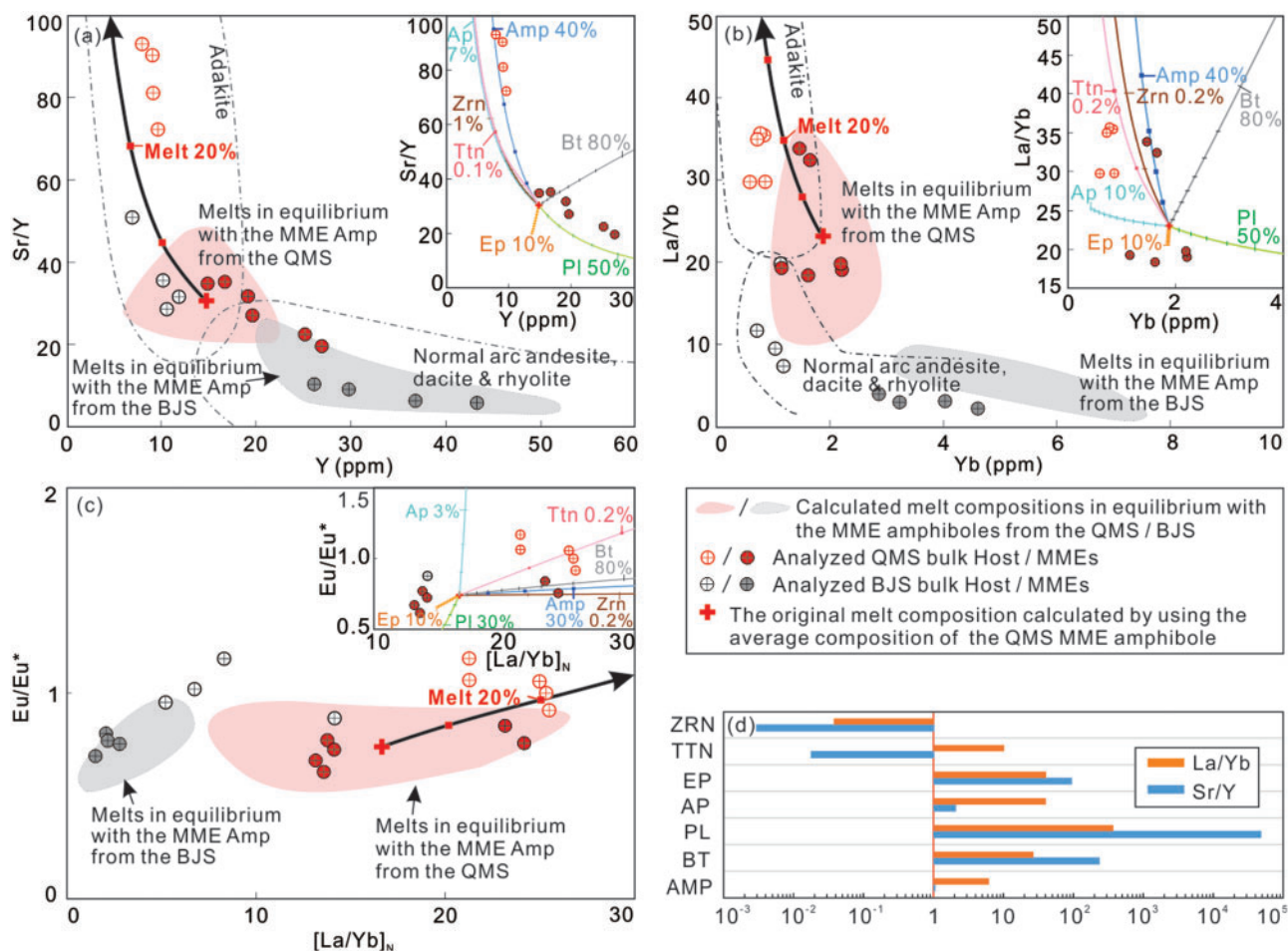
Fig. 13. Covariation diagrams for (a) Sr/Y vs Y, (b) La/Yb vs Yb, and (c) Eu/Eu* vs [La/Yb]$_N$ for melts in equilibrium with amphibole in MMEs of QMS (the red area) and BJS (the grey area) plutons. In (d), the average Sr/Y and La/Yb ratios of different minerals in the QMS MMEs are plotted for comparison, i.e., those lower than the original melt composition (Sr/Y = 30, La/Yb = 23) can effectively increase these two ratios in the residual melts. The original melt composition is calculated by using the average composition of amphibole in the QMS MMEs. (a-c) Also shown are modelling results for the evolution of the original melt initially in equilibrium with MME amphibole in the QMS pluton, assuming mineral modal abundances as in Table DR11 (25% amphibole + 45% plagioclase + 20% biotite + 1.7% apatite + 0.5% titanite + 2.4% epidote + 0.03% zircon). The insert diagrams in (a-c) show modelling results for the related Rayleigh fractional crystallization of various minerals. The parental magmas of the QMS pluton (the red area) clearly show higher Sr/Y and La/Yb ratios than those of the BJS pluton (the grey area), and are comparable to adakites. The fractionation of amphibole, titanite, and zircon further increases these two ratios and finally leads to the formation of the adakitic characteristics of the QMS host granitoids. The selected partition coefficient values are from Green *et al.* (1993), Hidalgo *et al.* (2007), Matsui (1977) and Klein *et al.* (1997), and are given in Table DR13. The discrimination lines in (a-b) are from Defant & Drummond (1990) and Richards & Kerrich (2007), respectively.

syn-collisional granitoids from the NQO, including both QMS and BJS granitoids, crystallized under similar conditions at upper crustal pressures of ~200 MPa and temperatures of 785–900 °C. Hence, the magmatic crystallization condition is not responsible for the different mineral fractionation in the QMS and BJS plutons. It may also be considered that titanite is likely to be crystallized in relatively oxidized rocks, but this crystallization process is actually accompanied by the stabilization of other minerals, for example the hydration of pyroxene to hornblende (7 Hedenbergite + 3 Ilmenite + 5 Quartz + 2 H$_2$O = 3 Titanite + 2 Fe-Actinolite; Frost *et al.,* 2000). However, neither pyroxene nor significant variations of ilmenite/magnetite modal abundances are observed in the QMS granitoids. In

addition, there is no clear difference in analysed loss-on-ignition values and hydrous mineral abundances between these two plutons, indicating their similar water/volatile contents. In fact, fractionation of titanite is thus primarily controlled by the melt composition (e.g., Front *et al.*, 2000; Seifert & Kramer, 2003); for example, titanite can crystallize only if it is on the liquidus in melt compositions with high Ti and Ca/Al ratios, with high Ca facilitating the stabilization of titanite (over ilmenite). Both QMS and BJS granitoids are metaluminous, supporting the formation of titanite (e.g., Frost *et al.*, 2000; Seifert & Kramer, 2003; Prowatke and Klemme, 2003), yet titanite is only found in the QMS granitoids. Considering that Ti is the requisite major component for titanite (CaTiSiO$_5$), the crystallization of titanite in

the QMS granitoids is thus most likely caused by the higher TiO$_2$ content of the parental melt, which is inherited from the source. This is also consistent with the noticeably higher TiO$_2$ content of the QMS granitoids than the BJS granitoids (e.g., 0.97 wt % in averaged QMS MME composition vs 0.65 wt % in averaged BJS MME composition). The high TiO$_2$ content in parental magmas facilitated the formation of titanite, the fractionation of which then further controlled the trace-element (REE, Y, Nb, Ta and others) systematics in the residual melts towards an adakitic signature.

Considering the highly variable composition of melts caused by the partial melting of the subducting/subducted ocean crust with varied compositions (e.g., Niu & Batiza, 1997), the ultimate control is the parental magma composition (major, minor and trace elements), which determines the mineralogy, phase equilibria and trace-element behaviour during magma evolution. Magmas parental to the QMS pluton with high TiO$_2$ content and Sr/Y and La/Yb ratios will finally evolve to melts with adakitic signatures after the titanite fractionation, whereas the non-adakitic compositions of the BJS granitoids may be attributed to lower Sr/Y and La/Yb ratios of their parental magmas and the absence of titanite as a result of low TiO$_2$ content. Therefore, parental magmas with high TiO$_2$ content, high Sr/Y and La/Yb ratios and their further fractionation of titanite due to this original composition are important characteristics of magmas evolving towards adakitic compositions, as represented by the QMS host granitoids. The potential role of parental magma compositional variation as a result of source compositional variation and the subsequent magma evolution in generating adakitic signature proposed here offer new insights into a better understanding of the widely debated petrogenesis of adakitic rocks.

CONCLUSIONS

In this study, we report major- and trace-element data on minerals from two well-characterized syn-collisional granitoid plutons in the NQO on the northern margin of the Tibetan Plateau in order to understand the petrogenesis of syn-collisional granitoids with MMEs, which allows us to test the hypothesis that continental collision zones are primary sites for net continental crustal growth.

(1) Different trace-element budgets in syn-collisional granitoids are systematically identified, and this forms the basis for understanding the effects of mineral fractionation on the compositional variation of the residual melt.

(2) Mineral chemistry further testifies that for both QMS and BJS plutons, MMEs are cumulates produced by earlier crystallization of the primitive andesitic melts, which originated from partial melting of subducting/subducted oceanic crust, whereas their host rocks represent the more evolved melt. Given that these syn-collisional granitoids represent juvenile continental crust, our studies support the hypothesis that continental collision zones are primary sites for net continental crust growth by partial melting of the subducted oceanic crust.

(3) The mineral compositional differences between QMS and BJS plutons indicate compositionally different parental magmas, corroborated by different compositions of the calculated melts in equilibrium with amphibole. We propose that parental magma composition with high TiO$_2$ content and high Sr/Y and La/Yb ratios exerts a primary control on the formation of adakite and adakitic rocks, as in the case of the QMS host granitoids. Among other factors, parental magma compositional variations resulting from magma-source compositional variations control the mineralogy, mineral chemistry and trace-element behaviour during subsequent magmatic evolution.

SUPPLEMENTARY DATA

Supplementary data are available at *Journal of Petrology* online.

Table DR1 Average bulk-rock compositions for MMEs and hosts from the BJS and QMS plutons in the eastern NQO (Chen *et al.*, 2015, 2016).

Table DR2 Operation conditions of LA-ICP-MS for the analysis of mineral compositions in this study.

Table DR3 Analytical results for amphibole in the BJS and QMS plutons using LA-ICP-MS.

Table DR4 Analytical results for biotite and muscovite in the BJS and QMS plutons using LA-ICP-MS.

Table DR5 Analytical results for plagioclase and orthoclase in the BJS and QMS plutons using LA-ICP-MS.

Table DR6 Analytical results for apatite in the BJS and QMS plutons using LA-ICP-MS.

Table DR7 Analytical results for epidote in the BJS and QMS plutons using LA-ICP-MS.

Table DR8 Analytical results for titanite in the BJS and QMS plutons using LA-ICP-MS.

Table DR9 Analytical results for carbonate and zircon in the BJS and QMS plutons using LA-ICP-MS.

Table DR10 Analytical results for zircon by Chen *et al.* (2015, 2016) in the BJS and QMS plutons using LA-ICP-MS.

Table DR11 Modelling mineral weight proportions and chemical element budgets in MMEs and host rocks of the QMS and BJS plutons.

Table DR12 Partition coefficients for several selected mineral pairs in our studied rocks.

Table DR13 Calculated compositions of the melts in equilibrium with amphibole, and partition coefficients between amphibole and melts used in this study.

Fig. DR1 Analytical accuracy (RE in %; a) and precision (RSD in %; b) of LA-ICP-MS analysis determined by a synthesized reference glass GSE-1G (Jochum *et al.*, 2005) as an unknown sample.

ACKNOWLEDGEMENTS

REFERENCES

Adam, J. & Green, T. H. (1994). The effects of pressure and temperature on the partitioning of Ti, Sr and REE between amphibole, clinopyroxene and basanitic melts. *Chemical Geology* **117**, 219–233.

Alonso-Perez, R., Müntener, O. & Ulmer, P. (2009). Igneous garnet and amphibole fractionation in the roots of island arcs: experimental constraints on andesitic liquids. *Contributions to Mineralogy and Petrology* **157**, 541.

Barbarin, B. (2005). Mafic magmatic enclaves and mafic rocks associated with some granitoids of the central Sierra Nevada batholith, California: nature, origin, and relations with the hosts. *Lithos* **80**, 155–177.

Barbarin, B. & Didier, J. (1992). Genesis and evolution of mafic microgranular enclaves through various types of interaction between coexisting felsic and mafic magmas. *Earth and Environmental Science Transactions of the Royal Society of Edinburgh* **83**, 145–153.

Belousova, E., Griffin, W., O'Reilly, S. Y. & Fisher, N. (2002a). Igneous zircon: trace element composition as an indicator of source rock type. *Contributions to Mineralogy and Petrology* **143**, 602–622.

Belousova, E. A., Griffin, W. L., O'Reilly, S. Y. & Fisher, N. I. (2002b). Apatite as an indicator mineral for mineral exploration: trace-element compositions and their relationship to host rock type. *Journal of Geochemical Exploration* **76**, 45–69.

Bottazzi, P., Tiepolo, M., Vannucci, R., Zanetti, A., Brumm, R., Foley, S. F. & Oberti, R. (1999). Distinct site preferences for heavy and light REE in amphibole and the prediction of Amph/LDREE. *Contributions to Mineralogy and Petrology* **137**, 36–45.

Browne, B. L., Eichelberger, J. C., Patino, L. C., Vogel, T. A., Uto, K. & Hoshizumi, H. (2006). Magma mingling as indicated by texture and Sr / Ba ratios of plagioclase phenocrysts from Unzen volcano, SW Japan. *Journal of Volcanology and Geothermal Research* **154**, 103–116.

Bruand, E., Storey, C. & Fowler, M. (2014). Accessory mineral chemistry of high Ba–Sr granites from northern Scotland: constraints on petrogenesis and records of whole-rock signature. *Journal of Petrology* **55**, 1619–1651.

Carmichael, I. S. (2002). The andesite aqueduct: perspectives on the evolution of intermediate magmatism in west-central (105–99°W) Mexico. *Contributions to Mineralogy and Petrology* **143**, 641–663.

Castillo, P. R. (2012). Adakite petrogenesis. *Lithos* **134–135**, 304–316.

Castillo, P. R., Janney, P. E. & Solidum, R. U. (1999). Petrology and geochemistry of Camiguin Island, southern Philippines: insights to the source of adakites and other lavas in a complex arc setting. *Contributions to Mineralogy and Petrology* **134**, 33–51.

Chambefort, I., Dilles, J. H. & Longo, A. A. (2013). Amphibole geochemistry of the Yanacocha Volcanics, Peru: evidence for diverse sources of magmatic volatiles related to gold ores. *Journal of Petrology* **54**, 1017–1046.

Chappell, B. W. (1996). Magma mixing and the production of compositional variation within granite suites: evidence from the granites of southeastern Australia. *Journal of Petrology* **37**, 449–470.

Chappell, B. W., White, A. J. R. & Wyborn, D. (1987). The importance of residual source material (restite) in granite petrogenesis. *Journal of Petrology* **28**, 1111–1138.

Chen, B., Chen, Z. C. & Jahn, B. M. (2009). Origin of mafic enclaves from the Taihang Mesozoic orogen, north China craton. *Lithos* **110**, 343–358.

Chen, B., Jahn, B.-M. & Suzuki, K. (2013). Petrological and Nd-Sr-Os isotopic constraints on the origin of high-Mg adakitic rocks from the North China Craton: tectonic implications. *Geology* **41**, 91–94.

Chen, S., Niu, Y., Li, J., Sun, W., Zhang, Y., Hu, Y. & Shao, F. (2016). Syn-collisional adakitic granodiorites formed by fractional crystallization: Insights from their enclosed mafic magmatic enclaves (MMEs) in the Qumushan pluton, North Qilian Orogen at the northern margin of the Tibetan Plateau. *Lithos* **248–251**, 455–468.

Chen, S., Niu, Y., Sun, W., Zhang, Y., Li, J., Guo, P. & Sun, P. (2015). On the origin of mafic magmatic enclaves (MMEs) in syn-collisional granitoids: evidence from the Baojishan pluton in the North Qilian Orogen, China. *Mineralogy and Petrology* **109**, 577–596.

Chen, S., Niu, Y. & Xue, Q. (2018). Syn-collisional felsic magmatism and continental crust growth: A case study from the North Qilian Orogenic Belt at the northern margin of the Tibetan Plateau. *Lithos* **308-309**, 53–64.

Chung, S.-L., Liu, D., Ji, J., Chu, M.-F., Lee, H.-Y., Wen, D.-J., Lo, C.-H., Lee, T.-Y., Qian, Q. & Zhang, Q. (2003). Adakites from continental collision zones: melting of thickened lower crust beneath southern Tibet. *Geology* **31**, 1021–1024.

Condie, K. C. (1998). Episodic continental growth and supercontinents. *Earth and Planetary Science Letters* **163**, 97–108.

Dahlquist, J. A. (2002). Mafic microgranular enclaves: early segregation from metaluminous magma (Sierra de Chepes), Pampean Ranges, NW Argentina. *Journal of South American Earth Sciences* **15**, 643–655.

Defant, M. J. & Drummond, M. S. (1990). Derivation of some modern arc magmas by melting of young subducted lithosphere. *Nature* **347**, 662–665.

Frost, B. R., Chamberlain, K. R. & Schumacher, J. C. (2000). Sphene (titanite): phase relations and role as a geochronometer. *Chemical Geology* **172**, 131–148.

Gao, S., Rudnick, R. L., Yuan, H.-L., Liu, X.-M., Liu, Y.-S., Xu, W.-L., Ling, W.-L., Ayers, J., Wang, X.-C. & Wang, Q.-H. (2004). Recycling lower continental crust in the North China craton. *Nature* **432**, 892–897.

Green, T. H., Adam, J. & Site, S. H. (1993). Proton microprobe determined trace element partition coefficients between pargasite, augite and silicate or carbonatitic melts. *EOS, Transactions of the American Geophysical Union* **74**, 340.

Hidalgo, P. J. & Rooney, T. O. (2010). Crystal fractionation processes at Baru volcano from the deep to shallow crust. *Geochemistry, Geophysics, Geosystems* **11**, Q12S30.

Hidalgo, S., Monzier, M., Martin, H., Chazot, G., Eissen, J.-P. & Cotten, J. (2007). Adakitic magmas in the Ecuadorian

Volcanic Front: petrogenesis of the Iliniza Volcanic Complex (Ecuador). *Journal of Volcanology and Geothermal Research* **159**, 366–392.

Hofmann, A. W. (1988). Chemical differentiation of the Earth: the relationship between mantle, continental crust, and oceanic crust. *Earth and Planetary Science Letters* **90**, 297–314.

Hoskin, P. W. O. & Schaltegger, U. (2003). The composition of zircon and igneous and metamorphic petrogenesis. *Reviews in Mineralogy and Geochemistry* **53**, 27–62.

Huang, H., Niu, Y. & Mo, X. (2016). Syn-collisional granitoids in the Qilian Block on the Northern Tibetan Plateau: a long-lasting magmatism since continental collision through slab steepening. *Lithos* **246–247**, 99–109.

Huang, H., Niu, Y., Nowell, G., Zhao, Z., Yu, X., Zhu, D.-C., Mo, X. & Ding, S. (2014). Geochemical constraints on the petrogenesis of granitoids in the East Kunlun Orogenic belt, northern Tibetan Plateau: implications for continental crust growth through syn-collisional felsic magmatism. *Chemical Geology* **370**, 1–18.

Huang, H., Niu, Y. & Mo, X. (2017). Garnet effect on Nd-Hf isotope decoupling: evidence from the Jinfosi batholith, Northern Tibetan Plateau. *Lithos* **274-275**, 31–38.

Huang, H., Niu, Y., Nowell, G., Zhao, Z., Yu, X., Mo, X. & Ding, S. (2015). The nature and history of the Qilian Block in the context of the development of the Greater Tibetan Plateau. *Gondwana Research* **28**, 209–224.

Jochum, K. P., Willbold, M., Raczek, I., Stoll, B. & Herwig, K. (2005). Chemical characterisation of the USGS reference glasses GSA-1G, GSC-1G, GSD-1G, GSE-1G, BCR-2G, BHVO-2G and BIR-1G using EPMA, ID-TIMS, ID-ICP-MS and LA-ICP-MS. *Geostandards and Geoanalytical Research* **29**, 285–302.

Klein, M., Stosch, H. G. & Seck, H. A. (1997). Partitioning of high field-strength and rare-earth elements between amphibole and quartz-dioritic to tonalitic melts: an experimental study. *Chemical Geology* **138**, 257–271.

Lin, J., Liu, Y., Yang, Y. & Hu, Z. (2016). Calibration and correction of LA-ICP-MS and LA-MC-ICP-MS analyses for element contents and isotopic ratios. *Solid Earth Sciences* **1**, 5–27.

Liu, L., Qiu, J.-S. & Li, Z. (2013). Origin of mafic microgranular enclaves (MMEs) and their host quartz monzonites from the Muchen pluton in Zhejiang Province, Southeast China: implications for magma mixing and crust–mantle interaction. *Lithos* **160–161**, 145–163.

Liu, Y., Hu, Z., Gao, S., Günther, D., Xu, J., Gao, C. & Chen, H. (2008). In situ analysis of major and trace elements of anhydrous minerals by LA-ICP-MS without applying an internal standard. *Chemical Geology* **257**, 34–43.

Macpherson, C. G., Dreher, S. T. & Thirlwall, M. F. (2006). Adakites without slab melting: high pressure differentiation of island arc magma, Mindanao, the Philippines. *Earth and Planetary Science Letters* **243**, 581–593.

Marks, M. A. W., Coulson, I. M., Schilling, J., Jacob, D. E., Schmitt, A. K. & Markl, G. (2008). The effect of titanite and other HFSE-rich mineral (Ti-bearing andradite, zircon, eudialyte) fractionation on the geochemical evolution of silicate melts. *Chemical Geology* **257**, 153–172.

Matsui, Y. (1977). Crystal structure control in trace element partition between crystal and magma. *Tectonics* **100**, 315–324.

McLeod, G. W., Dempster, T. J. & Faithfull, J. W. (2011). Deciphering magma-mixing processes using zoned titanite from the Ross of Mull granite, Scotland. *Journal of Petrology* **52**, 55–82.

Mo, X., Niu, Y., Dong, G., Zhao, Z., Hou, Z., Zhou, S. & Ke, S. (2008). Contribution of syncollisional felsic magmatism to continental crust growth: a case study of the Paleogene

Linzizong volcanic succession in southern Tibet. *Chemical Geology* **250**, 49–67.

Niu, Y. L. (2005). Generation and evolution of basaltic magmas: some basic concepts and a new view on the origin of Mesozoic-Cenozoic basaltic volcanism in Eastern China. *Geological Journal of China University* **11**, 9–46.

Niu, Y. L. & Batiza, R. (1997). Trace element evidence from seamounts for recycled oceanic crust in the Eastern Pacific mantle. *Earth and Planetary Science Letters* **148**, 471–483.

Niu, Y., Mo, X., Dong, G., Zhao, Z., Hou Z., Zhou S. & Ke, S. (2007). Continental collision zones are primary sites of net continental crustal growth: evidence from the Linzizong volcanic succession in Southern Tibet. *EOS Trans. AGU* **88**(52), Fall Meet., Suppl., Abstract V34A-01.

Niu, Y. L. & O'Hara, M. J. (2009). MORB mantle hosts the missing Eu (Sr, Nb, Ta and Ti) in the continental crust: new perspectives on crustal growth, crust–mantle differentiation and chemical structure of oceanic upper mantle. *Lithos* **112**, 1–17.

Niu, Y., Zhao, Z., Zhu, D.-C. & Mo, X. (2013). Continental collision zones are primary sites for net continental crust growth— A testable hypothesis. *Earth-Science Reviews* **127**, 96–110.

O' Nions, R. K., Evensen, N. M. & Hamilton, P. J. (1979). Geochemical modelling of mantle differentiation and crustal growth. *Journal of Geophysical Research* **84**, 6091–6101.

Piccoli, P., Candela, P. & Rivers, M. (2011). Interpreting magmatic processes from accessory phases: titanite—a small-scale recorder of large-scale processes. *Earth and Environmental Science Transactions of the Royal Society of Edinburgh* **91**, 257–267.

Ribeiro, J. M., Maury, R. C. & Grégoire, M. (2016). Are adakites slab melts or high-pressure fractionated mantle melts? *Journal of Petrology* **57**, 839–862.

Richards, J. P. & Kerrich, R. (2007). Special Paper: Adakite-like rocks: their diverse origins and questionable role in metallogenesis. *Economic Geology* **102**, 537–576.

Rodrĺguez, C., Sellés, D., Dungan, M., Langmuir, C. & Leeman, W. (2007). Adakitic dacites formed by intracrustal crystal fractionation of water-rich parent magmas at Nevado de Longaví volcano (36·2°S; Andean Southern Volcanic Zone, Central Chile). *Journal of Petrology* **48**, 2033–2061.

Rooney, T. O., Franceschi, P. & Hall, C. M. (2011). Water-saturated magmas in the Panama Canal region: a precursor to adakite-like magma generation? *Contributions to Mineralogy and Petrology* **161**, 373–388.

Seifert, W. & Kramer, W. (2003). Accessory titanite: an important carrier of zirconium in lamprophyres. *Lithos* **71**, 81–98.

Sha, L.-K. & Chappell, B. W. (1999). Apatite chemical composition, determined by electron microprobe and laser-ablation inductively coupled plasma mass spectrometry, as a probe into granite petrogenesis. *Geochimica et Cosmochimica Acta* **63**, 3861–3881.

Smith, M. P., Storey, C. D., Jeffries, T. E. & Ryan, C. (2009). In situ U–Pb and trace element analysis of accessory minerals in the Kiruna District, Norrbotten, Sweden: new constraints on the timing and origin of mineralization. *Journal of Petrology* **50**, 2063–2094.

Song, S., Niu, Y., Su, L., Wei, C. & Zhang, L. (2014a). Adakitic (tonalitic-trondhjemitic) magmas resulting from eclogite decompression and dehydration melting during exhumation in response to continental collision. *Geochimica et Cosmochimica Acta* **130**, 42–62.

Song, S., Niu, Y., Su, L. & Xia, X. (2013). Tectonics of the North Qilian orogen, NW China. *Gondwana Research* **23**, 1378–1401.

Song, S., Niu, Y., Su, L., Zhang, C. & Zhang, L. (2014b). Continental orogenesis from ocean subduction, continent collision/subduction, to orogen collapse, and orogen recycling: the example of the North Qaidam UHPM belt, NW China. *Earth-Science Reviews* **129**, 59–84.

Song, S., Niu, Y., Zhang, L. & Zhang, G. (2009). Time constraints on orogenesis from oceanic subduction to continental subduction, collision, and exhumation: an example from North Qilian and North Qaidam HP-UHP belts. *Acta Petrologica Sinica* **25**, 2067–2077.

Song, S., Zhang, L., Niu, Y., Su, L., Song, B. & Liu, D. (2006). Evolution from oceanic subduction to continental collision: a case study from the Northern Tibetan Plateau based on geochemical and geochronological data. *Journal of Petrology* **47**, 435–455.

Stern, R. J. & Scholl, D. W. (2010). Yin and yang of continental crust creation and destruction by plate tectonic processes. *International Geology Review* **52**, 1–31.

Streck, M. J., Leeman, W. P. & Chesley, J. (2007). High-magnesian andesite from Mount Shasta: a product of magma mixing and contamination, not a primitive mantle melt. *Geology* **35**, 351–354.

Sun, S.-S. & McDonough, W. F. (1989). Chemical and isotopic systematics of oceanic basalts: implications for mantle composition and processes. *Geological Society, London, Special Publications* **42**, 313–345.

Tang, G.-J., Wang, Q., Wyman, D. A., Chung, S.-L., Chen, H.-Y. & Zhao, Z.-H. (2017). Genesis of pristine adakitic magmas by lower crustal melting: a perspective from amphibole composition. *Journal of Geophysical Research: Solid Earth* **122**, 1934–1948.

Taylor, S. R. (1967). The origin and growth of continents. *Tectonophysics* **4**, 17–34.

Taylor S. R. (1977). Island arc models and the composition of the continental crust. In: Talwani M. & Pitman W. C. III (eds) *Island Arcs, Deep Sea Trenches, and Back-Arc Basins*. Maurice Ewing Ser., **1**, 325–335, Am. Geophys. Union, Washington, D.C.

Tiepolo, M., Langone, A., Morishita, T. & Yuhara, M. (2012). On the recycling of amphibole-rich ultramafic intrusive rocks in the arc crust: evidence from Shikanoshima Island (Kyushu, Japan). *Journal of Petrology* **53**, 1255–1285.

Tiepolo, M., Oberti, R. & Vannucci, R. (2002). Trace-element incorporation in titanite: constraints from experimentally determined solid/liquid partition coefficients. *Chemical Geology* **191**, 105–119.

Tseng, C.-Y., Yang, H.-J., Yang, H.-Y., Liu, D., Wu, C., Cheng, C.-K., Chen, C.-H. & Ker, C.-M. (2009). Continuity of the North Qilian and North Qinling orogenic belts, Central Orogenic System of China: evidence from newly discovered Paleozoic adakitic rocks. *Gondwana Research* **16**, 285–293.

Wang, Q., McDermott, F., Xu, J.-f., Bellon, H. & Zhu, Y.-t. (2005). Cenozoic K-rich adakitic volcanic rocks in the Hohxil area, northern Tibet: lower-crustal melting in an intracontinental setting. *Geology* **33**, 465–468.

Wang, Q., Wyman, D. A., Xu, J., Jian, P., Zhao, Z., Li, C., Xu, W., Ma, J. & He, B. (2007). Early Cretaceous adakitic granites in the Northern Dabie Complex, central China: implications for partial melting and delamination of thickened lower crust. *Geochimica et Cosmochimica Acta* **71**, 2609–2636.

Xia, L. Q., Xia, Z. C. & Xu, X. Y. (2003). Magmagenesis in the Ordovician backarc basins of the northern Qilian Mountains, China. *Geological Society of America Bulletin* **115**, 1510–1522.

Xia, X., Song, S. & Niu, Y. (2012). Tholeiite–boninite terrane in the North Qilian suture zone: implications for subduction initiation and back-arc basin development. *Chemical Geology* **328**, 259–277.

Xia, X. H. & Song, S. G. (2010). Forming age and tectono-petrogenises of the Jiugequan ophiolite in the North Qilian Mountain, NW China. *Chinese Science Bulletin* **55**, 1899–1907.

Xiao, Y., Niu, Y., Song, S., Davidson, J. & Liu, X. (2013). Elemental responses to subduction-zone metamorphism: constraints from the North Qilian Mountain, NW China. *Lithos* **160–161**, 55–67.

Yu, S., Zhang, J., Qin, H., Sun, D., Zhao, X., Cong, F. & Li, Y. (2015). Petrogenesis of the early Paleozoic low-Mg and high-Mg adakitic rocks in the North Qilian orogenic belt, NW China: implications for transition from crustal thickening to extension thinning. *Journal of Asian Earth Sciences* **107**, 122–139.

Zhang, Y., Niu, Y., Hu, Y., Liu, J., Ye, L., Kong, J. & Duan, M. (2016). The syncollisional granitoid magmatism and continental crust growth in the West Kunlun Orogen, China – Evidence from geochronology and geochemistry of the Arkarz pluton. *Lithos* **245**, 191–204.

Zhang, B., Hu, X., Li, P., Tang, Q. & Zhou, W. (2019). Trace element partitioning between amphibole and hydrous silicate glasses at 0.6-2.6 GPa. *Acta Geochim* **38**, 414–429.